

# Scalable control of mounting and attack by $Esr1^+$ neurons in the ventromedial hypothalamus

Hyosang Lee<sup>1,2</sup>, Dong-Wook Kim<sup>3</sup>, Ryan Remedios<sup>1</sup>, Todd E. Anthony<sup>1</sup>, Angela Chang<sup>1</sup>, Linda Madisen<sup>4</sup>, Hongkui Zeng<sup>4</sup> & David J. Anderson<sup>1,2,3</sup>

Social behaviours, such as aggression or mating, proceed through a series of appetitive and consummatory phases<sup>1</sup> that are associated with increasing levels of arousal<sup>2</sup>. How such escalation is encoded in the brain, and linked to behavioural action selection, remains an unsolved problem in neuroscience. The ventrolateral subdivision of the murine ventromedial hypothalamus (VMHvl) contains neurons whose activity increases during male–male and male–female social encounters. Non-cell-type-specific optogenetic activation of this region elicited attack behaviour, but not mounting<sup>3</sup>. We have identified a subset of VMHvl neurons marked by the oestrogen receptor 1 ( $Esr1$ ), and investigated their role in male social behaviour. Optogenetic manipulations indicated that  $Esr1^+$  (but not  $Esr1^-$ ) neurons are sufficient to initiate attack, and that their activity is continuously required during ongoing agonistic behaviour. Surprisingly, weaker optogenetic activation of these neurons promoted mounting behaviour, rather than attack, towards both males and females, as well as sniffing and close investigation. Increasing photostimulation intensity could promote a transition from close investigation and mounting to attack, within a single social encounter. Importantly, time-resolved optogenetic inhibition experiments revealed requirements for  $Esr1^+$  neurons in both the appetitive (investigative) and the consummatory phases of social interactions. Combined optogenetic activation

and calcium imaging experiments *in vitro*, as well as c-Fos analysis *in vivo*, indicated that increasing photostimulation intensity increases both the number of active neurons and the average level of activity per neuron. These data suggest that  $Esr1^+$  neurons in VMHvl control the progression of a social encounter from its appetitive through its consummatory phases, in a scalable manner that reflects the number or type of active neurons in the population.

To identify molecular markers for neurons that mediate aggression, we performed double-labelling experiments using markers for subsets of neurons in VMHvl<sup>4</sup>, and the neuronal activation marker c-Fos<sup>5</sup>, in resident males that had recently attacked an intruder. These studies identified  $Esr1$  (ref. 6) as enriched in cells activated during aggression (>80% of c-Fos<sup>+</sup> cells  $Esr1^+$ ; Extended Data Fig. 1h–v). To gain genetic access to these neurons, we generated a knock-in mouse line in which the *Cre* recombinase gene was targeted to the 3' end of the *Esr1* coding sequence in a gene-conserving manner (Fig. 1a, b). *In situ* hybridization for *Cre* messenger RNA revealed an expression pattern similar to that of *Esr1* mRNA (Fig. 1c–h). As in wild-type mice<sup>7</sup>, the expression of *Esr1-Cre* mRNA in VMHvl was higher in females than in males (Fig. 1g–j and Extended Data Fig. 1a–d). Anti- $Esr1$  antibody staining (Fig. 1i, j, s, u) indicated that the fraction of  $Esr1^+$  cells (~40%; see below) was similar in wild-type and gene-targeted mice.

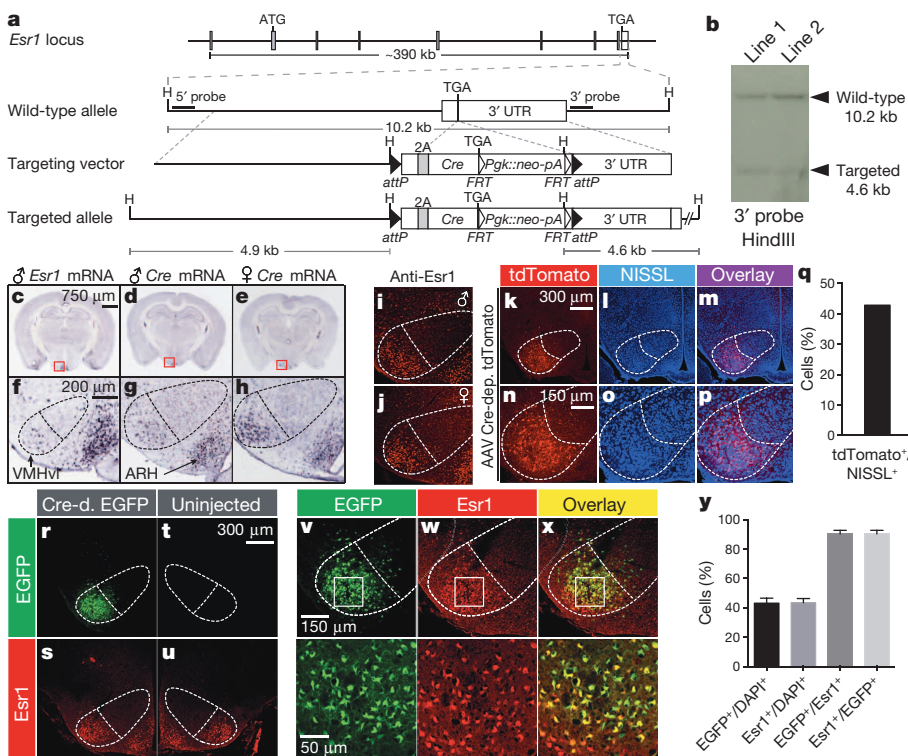


**Figure 1 | Generation and characterization of a knock-in mouse line expressing Cre recombinase in  $Esr1^+$  cells.** **a**, Strategy for targeting the *Esr1* locus. H, HindIII; 3' UTR, 3' untranslated region; 2A, F2A sequence; Pgk, phosphoglycerate kinase promoter; neo, neomycin-resistance gene; pA, polyadenylation signal. **b**, Southern blot of HindIII-digested genomic DNA from two correctly targeted *Esr1*<sup>cre/+</sup> embryonic stem cell lines. Wild-type (10.2 kb) and targeted (4.6 kb) alleles are revealed by a 3' probe (a). **c–h**, *In situ* hybridization for *Esr1* mRNA in wild-type male (c, f, ©2014 Allen Institute for Brain Science. Allen Mouse Brain Atlas [Internet]. Available from: <http://mouse.brain-map.org/experiment/show/79591677>, Bregma –1.75 mm) and for *Cre* mRNA in *Esr1*<sup>cre/+</sup> male (d, g) and female (e, h) mice (Bregma –1.65 mm). VMHvl, ventrolateral subdivision of the ventromedial hypothalamus; ARH, arcuate nucleus. Dotted outline indicates VMH. **i–x**, Immunostaining for *Esr1* protein (red) in wild-type (i, male; j, female) and *Esr1*<sup>cre/+</sup> female mice (s, u, w). **k–x**, Native fluorescence of *Cre*-dependent AAV-encoded markers in *Esr1*<sup>cre/+</sup> male (k–p, tdTomato) and female (r–x, EGFP) mice. Bottom panels in v–x are the boxed areas in top panels. **q, y**, Quantification of k–p (q, n = 1) and r–x (y, n = 4). Data are mean ± s.e.m. n = number of animals in this and all figures unless otherwise indicated.

<sup>1</sup>Division of Biology and Biological Engineering 156-29, California Institute of Technology, Pasadena, California 91125, USA. <sup>2</sup>Howard Hughes Medical Institute, Pasadena, California 91125, USA.

<sup>3</sup>Computation and Neural Systems, California Institute of Technology, Pasadena, California 91125, USA. <sup>4</sup>Allen Institute for Brain Science, Seattle, Washington 98103, USA.

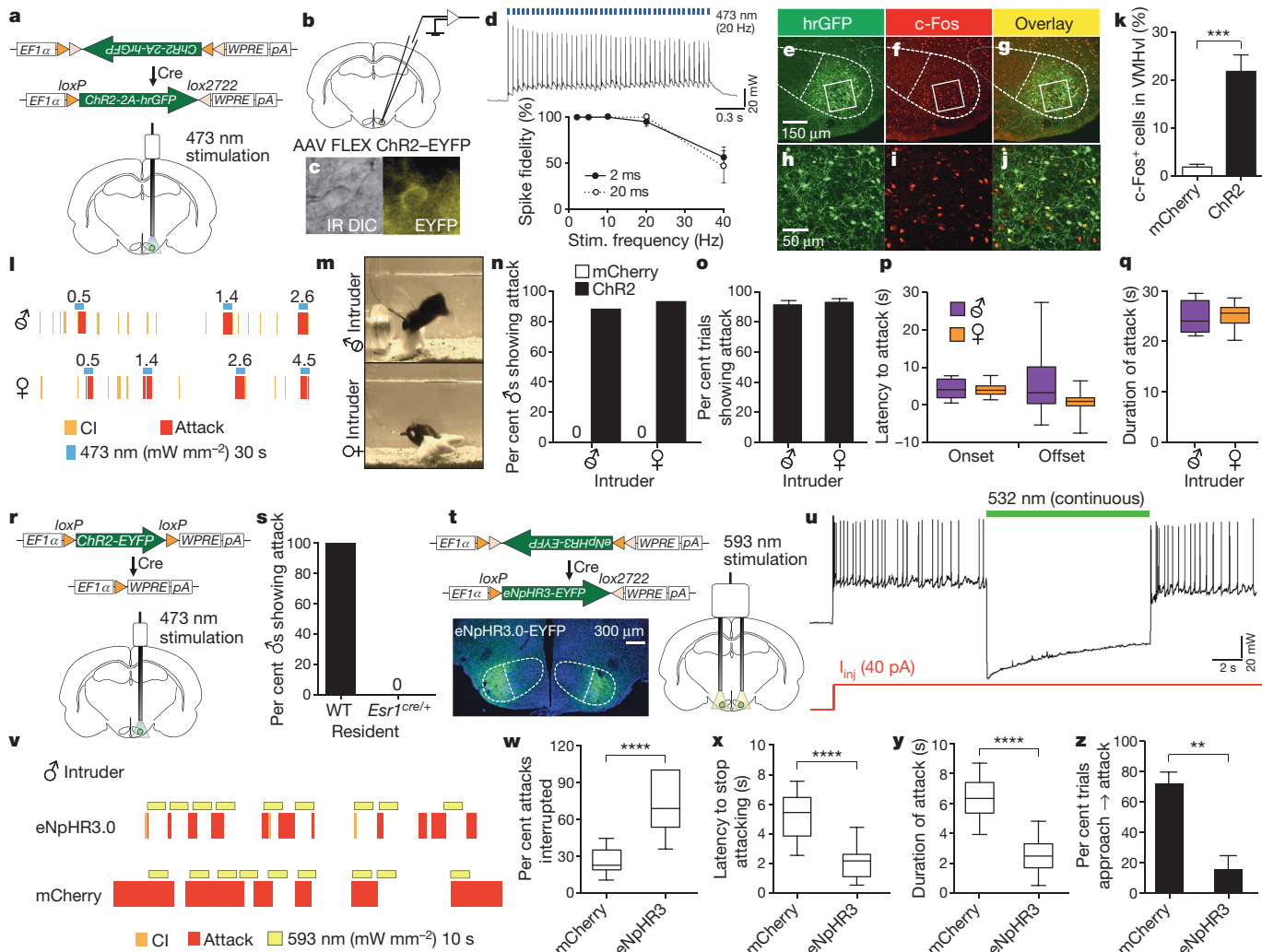


**Figure 2 |** *Esr1*<sup>+</sup> cells in VMHvl are necessary and sufficient for aggression. **a**, Strategy for optogenetic activation of *Esr1*<sup>+</sup> cells in VMHvl. *EF1 $\alpha$* , elongation factor 1 $\alpha$  promoter; *ChR2* is V5 epitope-tagged. **b-d**, Whole-cell patch-clamp recording from *Esr1*<sup>+</sup> cells in VMHvl (**c**, EYFP<sup>+</sup> cell) in acute hypothalamic slices. Photostimulation-evoked spiking (**d**, top) and quantification of spike fidelity (**d**, bottom) are shown (filled circles, 2 ms light pulse-width,  $n = 11$  cells; open circles, 20 ms pulse-width,  $n = 5$  cells). **e-j**, Double-labelling for Cre-dependent hrGFP viral reporter (**e**, **h**) and c-Fos (**f**, **i**) in VMHvl of *Esr1*<sup>cre/+</sup> males following photostimulation; **h-j**, boxed areas indicated in **e-g**. **k**, Quantification of **e-j** (mCherry,  $n = 5$ ; ChR2,  $n = 10$ ; \*\*\* $P < 0.001$ ; Mann-Whitney U-test). **l**, **m**, Representative raster plots (**l**) and video stills (**m**) illustrating photostimulation-evoked (blue bars;  $mW\ mm^{-2}$ ) attack (**l**, red) or close investigation (CI, yellow) by ChR2-expressing *Esr1*<sup>cre/+</sup> males (**m**, black mice), towards a castrated male (strike-through male symbol; **l**, **m**, upper) or an intact female (**l**, **m**, lower). See Supplementary Video 1. **n-q**, Quantification of attack parameters towards castrated males (ChR2,

**n**,  $n = 33$ ; **o**,  $n = 23$ ; **p**, **q**,  $n = 11$ ; mCherry, **n**,  $n = 14$ ) or females (ChR2, **n**,  $n = 28$ ; **o**,  $n = 22$ ; **p**, **q**,  $n = 16$ ; mCherry, **n**,  $n = 10$ ). **r**, Photoactivation of *Esr1*<sup>-</sup> cells using 'Cre-out' ChR2 AAV. **s**, Percentage of wild-type (WT;  $n = 4$ ) and *Esr1*<sup>cre/+</sup> ( $n = 9$ ) males showing photostimulated attack towards castrated males (see Extended Data Fig. 3b, c). **t**, Expression of eNpHR3.0 in VMHvl *Esr1*<sup>+</sup> neurons. **u**, Whole-cell patch-clamp recording in acute hypothalamic slices, showing photostimulation-induced suppression of current injection-evoked spiking in eNpHR3.0-mCherry expressing *Esr1*<sup>+</sup> cells. **v**, Representative raster plots illustrating effect of photostimulation on attack towards a male intruder. **w-y**, Quantification of behavioural parameters (mCherry,  $n = 10$ ; eNpHR3.0,  $n = 13$ ; \*\*\*\* $P < 0.0001$ ; Mann-Whitney U-test). **z**, Percentage of photostimulation trials in which approach to intruder led to attack (mCherry,  $n = 7$ ; eNpHR3,  $n = 4$ ; \*\* $P < 0.01$ ; Mann-Whitney U-test). Data are mean  $\pm$  s.e.m. (**d**, **k**, **o**, **z**) or median  $\pm$  min and maximum values (**p**, **q**, **w-y**).

Stereotaxic injection of recombinant adeno-associated viruses (AAVs) encoding Cre-dependent reporters into VMHvl of *Esr1*<sup>cre/+</sup> mice yielded marker-positive cells at a frequency ( $43.1 \pm 3.4\%$ , mean  $\pm$  s.e.m.) similar to that of *Esr1* expression ( $43.5 \pm 2.5\%$ ; Fig. 1k-y). Double-labelling experiments confirmed a high degree of overlap ( $\sim 90\%$ ) between recombinant marker<sup>+</sup> and *Esr1*<sup>+</sup> cells in VMHvl (Fig. 1v-y), without spillover into the arcuate nucleus (Extended Data Fig. 1e-g). To activate *Esr1*<sup>+</sup> neurons optogenetically, *Esr1*<sup>cre/+</sup> male mice were unilaterally injected in VMHvl with an AAV encoding a Cre-dependent channelrhodopsin 2 (ref. 8) and a nuclear humanized *Renilla* green fluorescent protein (hrGFP) reporter (Fig. 2a). Photostimulation-dependent activation of *Esr1*<sup>+</sup> neurons was confirmed *in vitro* using whole-cell patch-clamp recording in acute hypothalamic slices (Fig. 2b-d), and *in vivo* by

double-labelling for hrGFP and c-Fos (Fig. 2e-k), as well as by extracellular recordings (Extended Data Fig. 2).

Using an implanted fibre optic cable<sup>9</sup>, we tested the effect of optogenetic stimulation of VMHvl *Esr1*<sup>+</sup> neurons in resident males in their home cage under infrared light, using the resident-intruder assay<sup>10</sup>. Stimulation (20 Hz, 30 s, 20 ms pulse-width) elicited intense, time-locked attack towards both castrated male and female intruders (Fig. 2l, m), in over 87% of ChR2-expressing animals and in  $\sim 90\%$  of trials in those animals (Fig. 2n, o). Controls expressing Cre-dependent mCherry virus in VMHvl failed to show aggression during photostimulation (Fig. 2n, '0'; Extended Data Fig. 3a). Attack was initiated within  $\sim 5$  s of photostimulation when light pulses were delivered while the resident was facing the intruder and within one mouse body-length (Extended Data Fig. 4),

and continued through most of the 30-s stimulation period (Fig. 2p, q; Supplementary Video 1). Optogenetic stimulation of VMHvl  $Esr1^+$  neurons in females induced social investigation and occasional mounting, but not attack (Extended Data Fig. 5), indicating that sex differences in aggression probably occur within or downstream of VMHvl (refs 7, 11).

To determine whether non- $Esr1$ -expressing VMHvl neurons contribute to aggression, we injected an AAV in which Cre recombination excises the ChR2-EYFP (enhanced yellow fluorescent protein) coding sequence (Fig. 2r, 'Cre-out'). Photostimulation failed to elicit any attack behaviour in these mice, but did elicit attack behaviour in wild-type mice injected with the same virus (Fig. 2s and Extended Data Fig. 3b, c). Together, these data indicate that optogenetic activation of VMHvl  $Esr1^+$  neurons, but not of  $Esr1^-$  neurons, is sufficient and specific for attack.

Previous loss-of-function manipulations in VMHvl, including GluCl-mediated neuronal silencing<sup>9</sup>, ablation of progesterone receptor<sup>+</sup> neurons<sup>11</sup> and RNA interference-mediated knockdown of *Esr1* mRNA<sup>12</sup>, reduced aggression, but such manipulations required a time scale of days or weeks. Therefore they did not distinguish whether these neurons are required to sense conspecifics, for actual attack, or for both. To distinguish these possibilities, we performed time-resolved, reversible optogenetic inhibition of VMHvl  $Esr1^+$  neurons using eNpHR3.0<sup>13</sup>. Whole-cell patch-clamp recordings confirmed efficient photostimulation-dependent (532 nm) silencing of  $Esr1^+$  neurons (Fig. 2u). Bilateral silencing (10 s continuous illumination) during an agonistic encounter interrupted attack in <3 s in ~60% of stimulation trials, with a median attack duration of ~2 s (Fig. 2v–y). In some trials, ongoing attack was abrogated almost instantaneously by photostimulation (Supplementary Video 2). Photostimulation also prevented the initiation of attack, and sometimes caused retreat from the intruder (Supplementary Video 3), when delivered at the moment of approach (Fig. 2z).  $Esr1^{cre/+}$  males expressing mCherry showed no interruption of attack (Fig. 2v–y). Thus  $Esr1^+$  neuronal activity is required for both the initiation and continuation of attack.

At early stages of a social encounter, resident males exhibit close investigation of intruders, with sniffing of the ano-genital and head regions (Fig. 3a)<sup>14</sup>. Under conditions of weak ChR2 expression or low-intensity photostimulation, when attack was usually not evoked (see Fig. 4 and Extended Data Fig. 6), we observed an increase in both the average number and duration of close investigation episodes during 30 s photostimulation trials, irrespective of the sex of the intruder (Fig. 3c, d, solid vs open red bars). This phenotype was observed in females as well as males (Extended Data Fig. 5 and Supplementary Video 4). We also observed a more aggressive form of close investigation during photostimulation, in which the resident vigorously pushed his nose into the intruder's anogenital region, in ~25% of mice (Fig. 3e and Supplementary Video 5). Importantly, bilateral optogenetic inhibition using eNpHR3.0 interrupted ongoing close investigation in ~60% of resident males, vs <20% of controls (Fig. 3f). Thus, VMHvl  $Esr1^+$  neurons are necessary and sufficient for the investigative phase of a social encounter, as well as for attack.

Surprisingly, optogenetic stimulation under such conditions also promoted mounting behaviour, towards intact and castrated males as well as females (Fig. 3a, green rasters; Supplementary Videos 6 and 7, Extended Data Fig. 6) in ~50% of ChR2-expressing resident males and in ~60% of photostimulation trials for such males (Fig. 3g, h). Photostimulation of ChR2-expressing residents increased both the total number of mounts and average duration of mounting, towards both males and females (Fig. 3i, j). The frequency of evoked mounting was similar to that of control resident males towards female intruders (Fig. 3g, ♀, open bar). However when directed towards males, it was typically abortive and did not proceed to pelvic thrusting or ejaculation. Whereas male-directed mounting was only observed during photostimulation (Fig. 3a), its latency (~8–12 s; Fig. 3k) was longer than that for attack (~5 s). Photostimulation-induced mounting towards male intruders was not observed in mCherry-expressing controls (Fig. 3g, ♂, '0'). In

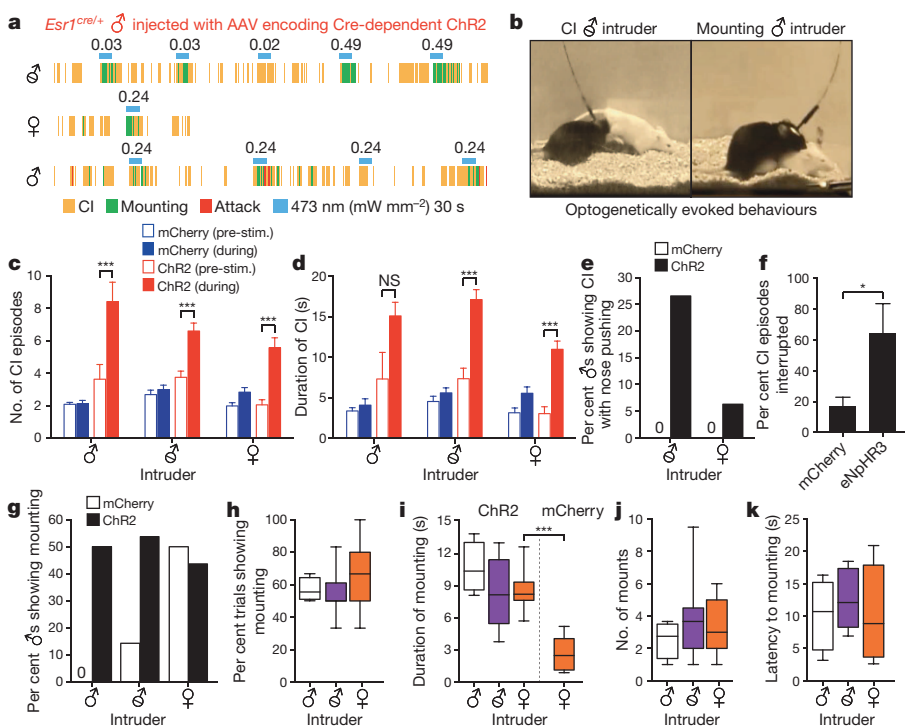


**Figure 3 |  $Esr1^+$  cells in VMHvl mediate close investigation (CI) and mounting behaviours.**

**a, b**, Representative raster plots (a) and video stills (b) illustrating photostimulation-evoked mounting (a, green; b, right) or CI (a, yellow; b, left) in ChR2-expressing  $Esr1^{cre/+}$  males towards intruders of the indicated sex. **c, d**, Number (c) and duration (d) of CI episodes performed by males expressing mCherry (blue bars) or ChR2 (red bars), before (open bars) or during (filled bars) photostimulation, towards intruder males ( $n = 4$  each), castrated males ( $n = 14$  and  $n = 18$ , respectively) or females ( $n = 10$  and  $n = 12$ ). \*\*\* $P < 0.001$ ; two-way ANOVA with Tukey's multiple comparisons test. **e**, Aggressive sniffing ('CI with nose pushing') during photostimulation by  $Esr1^{cre/+}$  males expressing mCherry (open bars) or ChR2 (filled bars) towards intruder castrated males ( $n = 14$  and  $n = 49$ , respectively) or females ( $n = 12$  and  $n = 32$ ). **f**, Percentage of CI episodes interrupted by photostimulation of  $Esr1^{cre/+}$  males expressing mCherry ( $n = 7$ ) or eNpHR3.0 ( $n = 3$ ). \* $P < 0.05$ ; Mann-Whitney U-test. **g**, Percentage of  $Esr1^{cre/+}$  males expressing mCherry (open bars) or ChR2 (filled bars) showing photostimulation-evoked mounting towards intruder males ( $n = 4$  and  $n = 8$ , respectively), castrated males ( $n = 14$  and  $n = 35$ ) or females ( $n = 10$  and  $n = 28$ ). **h–k**, Quantification of photostimulation-evoked mounting towards intruder males ( $n = 4$ ), castrated males ( $n = 11$ ) or intact females ( $n = 11$ ; i, mCherry,  $n = 5$ ) towards females. \*\*\* $P < 0.001$ ; Mann-Whitney U-test. Data are mean  $\pm$  s.e.m. (c, d) or median  $\pm$  minimum and maximum values (h–k).

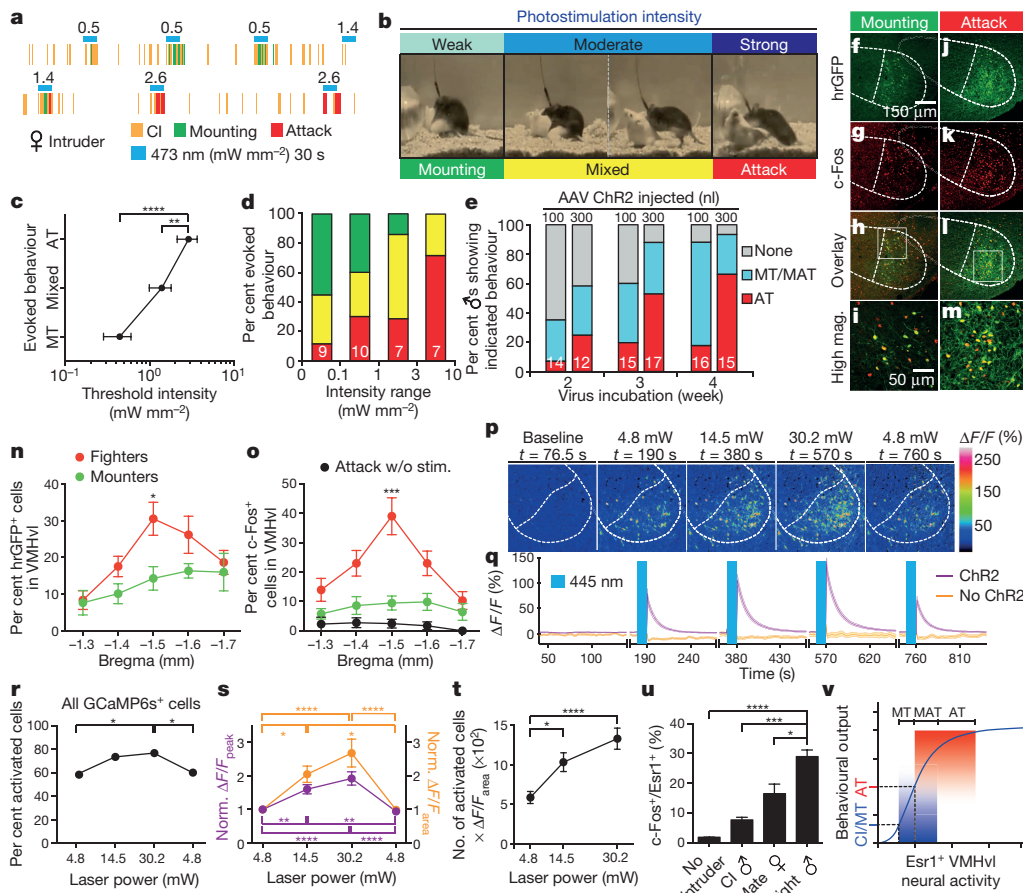


**Figure 4 | Behavioural responses shift from mounting to attack depending on photostimulation intensity and the number of activated cells in VMHvl.** **a, b**, Representative raster plots (a) and images (b) illustrating shift from mounting to attack with increasing photostimulation intensity. **c, d**, Threshold photostimulation intensities evoking mounting, mixed or attack behaviour (c,  $n = 11$ ), or the relative percentage of those behaviours evoked by the indicated intensity range (d,  $n$  in bars). Data are from test sessions exhibiting multiple behaviours. \*\* $P < 0.01$ , \*\*\* $P < 0.0001$ ; two-way ANOVA with Tukey's multiple comparisons test. **e**, Proportion of photostimulation-evoked behaviours in animals injected with different amounts of AAV (100 vs 300 nl), and incubated for different times post-injection (weeks).  $n$  within bars. Blue shading, mounting episodes with or without attack ('MT/MAT'). **f–m**, Double labelling for virally expressed hrGFP (f, j, h, i, l, m, native fluorescence) and photostimulation-induced c-Fos (g, k, i, m, anti-c-Fos, red) in solitary ChR2-expressing *Esr1*<sup>cre/+</sup> males photostimulated 1 h before euthanasia in their home cage, at an intensity that had previously evoked either mounting (f–i) or attack (j–m) several days earlier. **i, m**, Boxed areas in h and l, respectively. **n, o**, Quantification of number of hrGFP<sup>+</sup> (n) and c-Fos<sup>+</sup> (o) cells in VMHvl across successive axial levels, following solitary photostimulation of 'mounters' (green symbols,  $n = 6$ ) or 'attackers' (red symbols,  $n = 10$ ), as in f–m. Black symbols, no photostimulation before euthanasia ( $n = 3$ ). \* $P < 0.05$ ,

contrast, optogenetic inhibition did not interrupt ongoing male–female mounting, or reduce its duration or frequency (Extended Data Fig. 7 and Supplementary Note 1).

To characterize the conditions that evoked mounting vs attack, we manipulated the amount of virus injected; the incubation time; and the intensity and frequency of photostimulation (Fig. 4 and Extended Data Fig. 8). Mounting behaviour was typically observed after short (<3 weeks) incubation times following viral injection; when smaller amounts of virus were injected (100 vs 300 nl); or at lower stimulation intensities (Fig. 4a–e). In some animals, as the intensity of stimulation was increased during a single trial, evoked behaviours could be observed to switch from mounting only (Fig. 4a, b, d, green bars), to mixed mounting and attack (Fig. 4b, d, yellow bars) to attack only (Fig. 4a, b, d, red bars; Extended

\*\*\* $P < 0.001$ ; two-way ANOVA with Tukey's multiple comparisons test. **p–t**, Two-photon Ca<sup>2+</sup> imaging of acute hypothalamic slices expressing Cre-dependent ChR2-EYFP and Cre-independent GCaMP6s. **p**, Representative fluorescence images at the indicated time points and illumination power. **q**, Average Ca<sup>2+</sup> transients in GCaMP6s<sup>+</sup> cells with (purple trace,  $n = 60$ ) or without ChR2 (orange trace,  $n = 48$ ). Photostimulation (445 nm, 2-ms pulses, 20 Hz) was delivered for 10 s (blue bars in q). **r**, Percentage of GCaMP6s-expressing cells with  $\Delta F/F_{\text{peak}} > 5$  standard deviations from baseline, as a function of light power. \* $P < 0.05$ ; Pearson's Chi-square test. **s**, Normalized  $\Delta F/F_{\text{peak}}$  (purple) and  $\Delta F/F_{\text{area}}$  (orange, integrated area under the curves in q) during 30 s following photostimulation as a function of light power, relative to cells activated at 4.8 mW ( $n = 35$ ). **t**, Number of activated cells  $\times$  integrated activity per active cell, vs laser power. **s, t**, \* $P < 0.05$ , \*\* $P < 0.01$ , \*\*\* $P < 0.0001$ ; repeated measures one-way ANOVA. **u**, Percentage of c-Fos<sup>+</sup> cells among Esr1<sup>+</sup> neurons in VMHvl of wild-type animals following the indicated behaviours (control,  $n = 3$ ; CI,  $n = 4$ ; mate,  $n = 5$ ; fight,  $n = 5$ ). Data are mean  $\pm$  s.e.m.  $n$  = number of animals (c–e, n, o, u) or cells (q–s). **v**, Threshold model for relationship between level of Esr1<sup>+</sup> neuron activity and behaviour. MT, mount only; MAT, mixed mount and attack; AT, attack only. See also Supplementary Note 2.

Data Fig. 6d and Supplementary Videos 8–10). This effect often exhibited hysteresis: once attack was elicited, reducing the photostimulation intensity did not evoke mounting, but simply failed to elicit attack (Extended Data Fig. 9). A plot of log (photostimulation intensity) vs behaviour yielded a linear relationship, with mounting (either alone or mixed with attack) evoked up to 1.4 mW mm<sup>-2</sup> and attack (only) evoked by intensities  $> 3$  mW mm<sup>-2</sup> (Fig. 4c). Optogenetically evoked mounting vs attack behaviours were not strongly dependent on the frequency of photostimulation, although a higher percentage of stimulation trials elicited attack at 20 Hz than at 10 Hz (Extended Data Fig. 8).

The observation that the frequency of optogenetically evoked attack was higher in animals injected with larger volumes of virus (Fig. 4e, 300 nl) indicated that attack required activation of a larger number of

*Esr1<sup>+</sup>* neurons. Indeed, mice in which photostimulation induced attack contained a significantly higher number of virally infected (*hrGFP<sup>+</sup>*) cells in VMHvl, than did animals in which it evoked mounting (Fig. 4f, j, n). Moreover, photostimulation of solitary residents 1 h before euthanasia yielded a significantly higher number of c-Fos<sup>+</sup> cells within the ChR2-expressing (*hrGFP<sup>+</sup>*) population in ‘attackers’ ( $80.5 \pm 4.9\%$ , mean  $\pm$  s.e.m.) than in ‘mounters’ ( $54.7 \pm 12.6\%$ ,  $P < 0.05$ , two-tailed Student’s *t*-test; Fig. 4f–m, o). These data indicate that optogenetically evoked attack requires a larger number of ChR2-expressing and active *Esr1<sup>+</sup>* cells, than does mounting. Consistent with this conclusion, the percentage of c-Fos<sup>+</sup> cells among *Esr1<sup>+</sup>* neurons in wild-type, unmanipulated animals was significantly higher following naturally occurring fighting, than after mating or close investigation (Fig. 4u)<sup>3</sup>.

To investigate within the same preparation the relationship between the intensity of photostimulation and the number of active neurons in VMHvl, we used calcium imaging with a genetically encoded calcium indicator, GCaMP6s<sup>15</sup>, to measure the extent of optogenetic activation in acute hypothalamic slices from *Esr1<sup>cre/+</sup>* males expressing ChR2 (Fig. 4p, q). Increasing the laser power over an approximately sixfold range significantly increased the fraction of GCaMP6s<sup>+</sup> cells exhibiting photostimulation-induced calcium transients (Fig. 4r), and also increased the peak and average activity per cell among neurons activated at the lowest power tested (Fig. 4q, s). There was a roughly linear relationship between laser power and overall activity (number of active neurons  $\times$  average activity/neuron), with a slope of about 30 (Fig. 4t). No response was observed in controls lacking ChR2 (Fig. 4q, orange traces). Thus increasing light intensity augmented both the number of active neurons, and the average level of activity per neuron.

Earlier studies revealed that VMHvl contains neurons activated during male aggression, whose optogenetic stimulation or pharmacogenetic inhibition<sup>16</sup> evoked or inhibited attack, respectively<sup>3</sup>. However, those studies used ubiquitous promoters, and therefore did not identify the subpopulation of neurons responsible for attack. Here we identify these neurons as a subset (~40%) of VMHvl cells expressing *Esr1*. From one perspective, it is incidental that this marker encodes a hormone receptor. Indeed, our knock-in mice were designed to permit functional manipulations of these neurons without perturbing *Esr1* function. Nevertheless, numerous genetic and pharmacologic studies have demonstrated steroid hormonal influences on the developmental and adult control of social behaviours, including those exerted via VMH<sup>12,17–20</sup> (reviewed in refs 21–23). However, relatively little is known about the circuit-level function of the neurons that express these receptors<sup>24</sup>. Genetic ablation of a closely related population of cells expressing the progesterone receptor partially reduced both male mating and aggression<sup>11</sup>, but such loss-of-function manipulations do not have the temporal resolution of optogenetics. To our knowledge, therefore, the present experiments are the first to report time-resolved gain- and loss-of-function manipulations of hypothalamic neurons that express a sex-steroid hormone receptor. They reveal a complex and dynamic relationship between neuronal activity in this population and social behaviour. The relationship of this activity to hormonal influences remains to be investigated.

Previous *in vivo* recordings and c-Fos analysis revealed that VMHvl also contains neurons activated during male–female encounters; however, no effects of functional perturbations on male mating behaviour were observed<sup>3</sup> (see Supplementary Note 1). Those studies were, therefore, compatible with the view that VMHvl contains ‘command’-like neurons<sup>25</sup> that control attack<sup>26</sup>, and that the female-activated neurons might even serve to inhibit such attack neurons during mating<sup>27</sup>. The experiments reported here suggest a rather different view of VMHvl function. They show that *Esr1<sup>+</sup>* neurons control different behaviours throughout the entire progression of a social interaction, from its appetitive through its consummatory phases<sup>1</sup>. The fact that these behaviours are evoked by optogenetic activation at low and high photostimulation intensities, respectively, further suggests that increasing activity in VMHvl, as the intensity of the social encounter escalates<sup>3</sup>, leads to qualitatively different behavioural outputs (Fig. 4v).

Several models may explain how such an apparent intensity coding of social behaviour is implemented at the cellular level (Supplementary Note 2). These include different subpopulations of *Esr1<sup>+</sup>* neurons with different activation thresholds, graded changes in activity within a single population (Extended Data Fig. 10), or more complex models involving attractor dynamics<sup>28</sup>. Although further experiments will be required to distinguish these possibilities, *in vivo* recordings revealed a substantial degree of overlap between neurons activated during mating vs fighting<sup>3</sup>. Whatever the explanation, the data suggest that *Esr1<sup>+</sup>* neurons in VMHvl may comprise a node in which a graded variable, perhaps representing the level of social arousal or cumulative sensory input, is transformed into differences in action selection at different thresholds. How this transformation occurs will be an interesting subject for future study.

**Note added in proof:** A detailed quantitative analysis of VMHvl spiking activity during male–male social interactions (Falkner *et al.*, *J. Neurosci.*, in the press) reveals that many individual neurons are active during both social investigation and attack; that spiking activity ramps up during the transition from investigation to attack; and that higher spiking activity during investigation predicts an increased likelihood of transitioning to attack. These results are consistent with the optogenetic experiments reported here.

## METHODS SUMMARY

**Generation of *Esr1<sup>cre</sup>* knock-in mice.** *Esr1<sup>cre</sup>* knock-in mice were generated from 129S6/EvSvTac embryonic stem cells by targeting the 3' end of the *Esr1* coding sequence with a cassette consisting of an F2A sequence, a *Cre* recombinase coding sequence, and an *Frt*-flanked PGK-neomycin resistance as an in-frame fusion. Chimaeric animals were backcrossed ( $n > 6$ ) to C57BL/6N. The *Frt*-flanked PGK-neopoly A cassette was removed by crossing *Esr1<sup>cre/+</sup>* mice to transgenic mice expressing flippase (FLPo, Jackson Laboratory, Stock No. 011065). The *Esr1<sup>cre</sup>* knock-in mice are available from the Jackson Laboratory (Stock No. 017911).

**Optogenetic activation and silencing of *Esr1<sup>+</sup>* neurons in VMHvl.** Adult *Esr1<sup>cre/+</sup>* male and female mice at ages between 2 to 4 months were stereotactically injected into the VMHvl with an AAV encoding Cre-dependent effector molecule (ChR2 or eNpHR3.0) or control fluorescent protein (mCherry, tdTomato or EGFP) following the procedures described previously<sup>3</sup>. After a 2–4-week recovery period, the virus-injected animals were examined behaviourally in their home cage using the resident–intruder assay for the next 2 to 5 weeks (1–2 test sessions per week). Photostimulation (ChR2, 473 nm, 20-ms pulses; eNpHR3.0, 593 nm, continuous) was applied to the virus-injected *Esr1<sup>cre/+</sup>* mice during social encounters with intruders (intact male, castrated male, or intact non-hormone primed female) 5–15 times per intruder.

All animal experiments were carried out in accordance with NIH guidelines and approved by the Institutional Animal Care and Use Committee (IACUC) at Caltech.

**Electrophysiological recordings and calcium imaging.** Whole-cell current clamp recordings and GCaMP6s-mediated two-photon calcium imaging were performed on acute hypothalamic slices prepared from virus-injected adult *Esr1<sup>cre/+</sup>* mice following the protocols described previously<sup>3,29,30</sup>. *In vivo* electrophysiology was performed as described<sup>3</sup>, using a modification of the 16-wire electrode bundle with an integrated optic fibre.

**Online Content** Any additional Methods, Extended Data display items and Source Data are available in the online version of the paper; references unique to these sections appear only in the online paper.

Received 4 September 2013; accepted 21 February 2014.

Published online 16 April 2014.

1. Tinbergen, N. in *Physiological Mechanisms in Animal Behaviour* Vol. IV *Symposia of the Society for Experimental Biology* 305–312 (Academic Press, 1950).
2. Devidze, N., Lee, A., Zhou, J. & Pfaff, D. CNS arousal mechanisms bearing on sex and other biologically regulated behaviors. *Physiol. Behav.* **88**, 283–293 (2006).
3. Lin, D. *et al.* Functional identification of an aggression locus in the mouse hypothalamus. *Nature* **470**, 221–226 (2011).
4. Lein, E. S. *et al.* Genome-wide atlas of gene expression in the adult mouse brain. *Nature* **445**, 168–176 (2007).
5. Morgan, J. I., Cohen, D. R., Hempstead, J. L. & Curran, T. Mapping patterns of c-fos expression in the central nervous system after seizure. *Science* **237**, 192–197 (1987).
6. Walter, P. *et al.* Cloning of the human estrogen receptor cDNA. *Proc. Natl Acad. Sci. USA* **82**, 7889–7893 (1985).

7. Xu, X. et al. Modular genetic control of sexually dimorphic behaviors. *Cell* **148**, 596–607 (2012).
8. Boyden, E. S., Zhang, F., Bamberg, E., Nagel, G. & Deisseroth, K. Millisecond-timescale, genetically targeted optical control of neural activity. *Nature Neurosci.* **8**, 1263–1268 (2005).
9. Aravanis, A. M. et al. An optical neural interface: *in vivo* control of rodent motor cortex with integrated fiberoptic and optogenetic technology. *J. Neural Eng.* **4**, S143–S156 (2007).
10. Blanchard, D. C. & Blanchard, R. J. Ethoexperimental approaches to the biology of emotion. *Annu. Rev. Psychol.* **39**, 43–68 (1988).
11. Yang, C. F. et al. Sexually dimorphic neurons in the ventromedial hypothalamus govern mating in both sexes and aggression in males. *Cell* **153**, 896–909 (2013).
12. Sano, K., Tsuda, M. C., Musatov, S., Sakamoto, T. & Ogawa, S. Differential effects of site-specific knockout of estrogen receptor alpha in the medial amygdala, medial pre-optic area, and ventromedial nucleus of the hypothalamus on sexual and aggressive behavior of male mice. *Eur. J. Neurosci.* **37**, 1308–1319 (2013).
13. Gradinariu, V. et al. Molecular and cellular approaches for diversifying and extending optogenetics. *Cell* **141**, 154–165 (2010).
14. Blanchard, R. J., Wall, P. M. & Blanchard, D. C. Problems in the study of rodent aggression. *Horm. Behav.* **44**, 161–170 (2003).
15. Chen, T. W. et al. Ultrasensitive fluorescent proteins for imaging neuronal activity. *Nature* **499**, 295–300 (2013).
16. Lerchner, W. et al. Reversible silencing of neuronal excitability in behaving mice by a genetically targeted, ivermectin-gated Cl<sup>-</sup> channel. *Neuron* **54**, 35–49 (2007).
17. Cohen, R. S. & Pfaff, D. W. Ventromedial hypothalamic neurons in the mediation of long-lasting effects of estrogen on lordosis behavior. *Prog. Neurobiol.* **38**, 423–453 (1992).
18. Musatov, S., Chen, W., Pfaff, D. W., Kaplitt, M. G. & Ogawa, S. RNAi-mediated silencing of estrogen receptor  $\alpha$  in the ventromedial nucleus of hypothalamus abolishes female sexual behaviors. *Proc. Natl Acad. Sci. USA* **103**, 10456–10460 (2006).
19. Spiteri, T. et al. Estrogen-induced sexual incentive motivation, proceptivity and receptivity depend on a functional estrogen receptor alpha in the ventromedial nucleus of the hypothalamus but not in the amygdala. *Neuroendocrinology* **91**, 142–154 (2010).
20. Spiteri, T. et al. The role of the estrogen receptor alpha in the medial amygdala and ventromedial nucleus of the hypothalamus in social recognition, anxiety and aggression. *Behav. Brain Res.* **210**, 211–220 (2010).
21. Simerly, R. B. Wired for reproduction: organization and development of sexually dimorphic circuits in the mammalian forebrain. *Annu. Rev. Neurosci.* **25**, 507–536 (2002).
22. Morris, J. A., Jordan, C. L. & Breedlove, S. M. Sexual differentiation of the vertebrate nervous system. *Nature Neurosci.* **7**, 1034–1039 (2004).
23. Wu, M. V. & Shah, N. M. Control of masculinization of the brain and behavior. *Curr. Opin. Neurobiol.* **21**, 116–123 (2011).
24. Kow, L. M., Easton, A. & Pfaff, D. W. Acute estrogen potentiates excitatory responses of neurons in rat hypothalamic ventromedial nucleus. *Brain Res.* **10**, 124–131 (2005).
25. Bentley, D. & Konishi, M. Neural control of behavior. *Annu. Rev. Neurosci.* **1**, 35–59 (1978).
26. Kruk, M. R. et al. Discriminant analysis of the localization of aggression-inducing electrode placements in the hypothalamus of male rats. *Brain Res.* **260**, 61–79 (1983).
27. Anderson, D. J. Optogenetics, sex, and violence in the brain: implications for psychiatry. *Biol. Psychiatry* **71**, 1081–1089 (2011).
28. Kristan, W. B. Neuronal decision-making circuits. *Curr. Biol.* **18**, R928–R932 (2008).
29. Haubensak, W. et al. Genetic dissection of an amygdala microcircuit that gates conditioned fear. *Nature* **468**, 270–276 (2010).
30. Vrontou, S., Wong, A. M., Rau, K. K., Koerber, H. R. & Anderson, D. J. Genetic identification of C fibres that detect massage-like stroking of hairy skin *in vivo*. *Nature* **493**, 669–673 (2013).

**Supplementary Information** is available in the online version of the paper.

**Acknowledgements** We thank C. Park for behavioural scoring, R. Robertson for behavioural scoring and MATLAB programming, L. Lo for testing Cre-mediated recombination in *Esr1<sup>cre/+</sup>* male mice, C. Chiu and X. Wang for histology, M. McCordle for genotyping, J. S. Chang for technical assistance, S. Pease for generation of knock-in mice, H. Cai for training in slice electrophysiology, A. Wong for assistance with two-photon imaging, K. Deisseroth and J. Harris for AAV constructs, E. Boyden for advice on ferrule fibre fabrication, D. Lin and M. Boyle for their contributions to early stages of this project, W. Hong and R. Axel for comments on the manuscript, C. Chiu for laboratory management and G. Mancuso for administrative assistance. D.J.A. is an Investigator of the Howard Hughes Medical Institute and a Paul G. Allen Distinguished Investigator. This work was supported in part by NIH grant no. R01MH070053, and grants from the Gordon Moore Foundation and Ellison Medical Research Foundation. H.L. was supported by the NIH Pathway to Independence Award 1K99NS074077. T.E.A. was supported by NIH NRSA postdoctoral fellowship grant 1F32HD055198-01 and a Beckman Fellowship.

**Author Contributions** H.L. characterized *Esr1<sup>cre</sup>* mice, designed and performed optogenetic behavioural experiments and co-wrote the manuscript; D.-W.K. performed slice electrophysiology and imaging experiments; R.R. performed *in vivo* electrophysiology; T.E.A. generated the *Esr1<sup>cre</sup>* targeting construct and AAV vectors; A.C. carried out some behavioural experiments; L.M. and H.Z. performed *in situ* hybridization experiments; D.J.A. supervised experiments and co-wrote the manuscript.

**Author Information** Reprints and permissions information is available at [www.nature.com/reprints](http://www.nature.com/reprints). The authors declare no competing financial interests. Readers are welcome to comment on the online version of the paper. Correspondence and requests for materials should be addressed to D.J.A. ([wuwei@caltech.edu](mailto:wuwei@caltech.edu)).

## METHODS

**Animals.** All experimental procedures involving use of live animals or their tissues were carried out in accordance with the NIH guidelines and approved by the Institutional Animal Care and Use Committee at California Institute of Technology (Caltech). Wild-type mice were purchased from Charles River Laboratories, Jackson Laboratory and Taconic. Animals were group-housed in ventilated cages in a temperature-controlled environment (23 °C), at humidity between 30 and 70%, with a 12-h light and 12-h dark cycle. Mice had *ad libitum* access to food and water. Mouse cages were changed weekly.

**Generation of *Esr1*<sup>cre</sup> knock-in mice.** *Esr1*<sup>cre</sup> knock-in mice were generated at Caltech Genetically Engineered Mouse Services core facility, following standard procedures. The targeting vector was designed to insert an *F2A* sequence, a *Cre* recombinase coding sequence, and an *Fr*t-flanked PGK-neomycin resistance cassette at the 3' end of *Esr1* coding sequence by homologous recombination as an in-frame fusion. Following electroporation of the targeting construct into 129S6/EvSvTac-derived TC-1 embryonic stem cells (gift of P. Leder), correctly targeted embryonic stem cells were selected by neomycin resistance and identified by genotyping PCR with the following primer sets: 5' arm primers (5.5 kb), 5'-gaccagccaccaggaaagctg-3' and 5'-cggtcgatgcacgatggatc-3'; 3' arm primers (3.1 kb), 5'-tcccgattcgcagcgc atcgc-3' and 5'-ttggggacatgcataagggc-3'. The positive embryonic stem cells were further confirmed by Southern blot analysis using the following probes: 5' probe, HindIII, 10.2 kb (wild-type allele) and 4.9 kb (targeted allele); 3' probe, HindIII, 10.2 kb (wild-type allele) and 4.6 kb (targeted allele); Cre probe, AflII, 7.2 kb. The probes were generated with the following primer sets: 5' probe, 5'-cacacgtttagctgtatgatgatc-3' and 5'-caggacaaaatgtggggatc-3'; 3' probe, 5'-gcagagatattgcgtggaa gg-3' and 5'-gccaatttgatcttgtcatccaag-3'; Cre probe, 5'-gtcaattttactgaccgtacacc-3' and 5'-ctaattccatcttcacagc-3'. Embryonic stem cells were then injected into recipient C57BL/6N blastocysts to generate chimaeric males that were then bred with C57BL/6N females. The *Fr*t-flanked PGK-*neo*-poly A cassette was removed by crossing *Esr1*<sup>cre/+</sup> mice to transgenic mice expressing flippase (Jackson Laboratory, Stock No. 011065)<sup>31</sup>. The flippase transgene was eliminated by backcrossing *Esr1*<sup>cre/+flippase</sup> mice to C57BL/6N for >6 generations. Genotype of the mice was determined by PCR on tail genomic DNA with the following primer sets: wild-type allele (598 bp) 5'-tggccactactagaaggactgtgg-3' and 5'-ggaggaatgaaaatacgtggacaatgtccc-3'; targeted allele (500 bp) 5'-agccgtctgggggtca-3' and 5'-agaaaacgcctggcgtatccc-3'; Cre (320 bp), 5'-gttgcagaacatgtggaca-3' and 5'-ctagacgtttgcacgttc-3'. The *Esr1*<sup>cre</sup> knock-in mice are available from the Jackson Laboratory (Stock No. 017911).

**Virus.** AAV.EF1 $\alpha$ .FLEX.ChR2-EYFP.WPRE and AAV.EF1 $\alpha$ .FLEX.eNpHR3.0-EYFP.WPRE were gifts of K. Deisseroth. AAV.hSynapsin.FLEX.tdTomato-2A-EGFP-Synaptophysin.WPRE and AAV.CAG.FLEX.EGFP.WPRE were gifts of J. Harris. AAV.EF1 $\alpha$ .FLEX.ChR2-V5-F2A-nuclear hrGFP.WPRE, AAV.EF1 $\alpha$ .lox.P.ChR2-EYPF.lox.P.WPRE and AAV.EF1 $\alpha$ .FLEX.mCherry.WPRE were generated in our laboratory. The viruses were prepared by the University of Pennsylvania Vector Core (AAV2.EF1 $\alpha$ .FLEX.ChR2-EYFP.WPRE, 2.0  $\times$  10<sup>13</sup> genomic copies per ml; AAV2.EF1 $\alpha$ .FLEX.ChR2-V5-F2A-nuclear hrGFP.WPRE, 2.2  $\times$  10<sup>12</sup> genomic copies per ml; AAV2.EF1 $\alpha$ .FLEX.mCherry.WPRE, 3.7  $\times$  10<sup>12</sup> genomic copies per ml; AAV2.EF1 $\alpha$ .lox.P.ChR2-EYPF.lox.P.WPRE, 1.8  $\times$  10<sup>12</sup> genomic copies per ml; AAV1.CAG.FLEX.EGFP.WPRE, 8  $\times$  10<sup>12</sup> genomic copies per ml), the Harvard Gene Therapy Initiative (AAV2.EF1 $\alpha$ .FLEX.eNpHR3.0-EYFP.WPRE, 4.2  $\times$  10<sup>12</sup> genomic copies per ml), and the University of North Carolina Gene Therapy Center (AAV1.hSynapsin.FLEX.tdTomato-2A-EGFP-Synaptophysin.WPRE, 6  $\times$  10<sup>12</sup> genomic copies per ml; AAV2.EF1 $\alpha$ :FLEX.eNpHR3.0-mCherry.WPRE, 3  $\times$  10<sup>12</sup> genomic copies per ml).

**Surgery.** Adult *Esr1*<sup>cre/+</sup> mice at ages between 2 to 4 months (sexually inexperienced) were housed individually for 5 days to 2 weeks in a reverse light/dark cycle room, and then stereotactically injected with a virus as described previously<sup>32</sup>. Briefly, animals were anaesthetized with isoflurane (0.8–5%) and placed in a stereotaxic frame (David Kopf Instruments). A virus was injected into VMHvl in either one or both hemispheres using a pulled glass capillary (World Precision Instruments) either by nanolitre pressure injection at a flow rate of 30 nl min<sup>-1</sup> (Micro4 controller, World Precision Instruments; Nanoject II, Drummond Scientific) or iontophoresis at 3  $\mu$ A for 5–10 min (7 s on and 7 s off, Midgard Precision Current Source, Stoelting)<sup>33</sup>. Stereotactic injection coordinates to target the VMHvl were obtained from either the Paxinos and Franklin atlas (AP: -1.5, ML:  $\pm$  0.78, DV: -5.75 mm) or the three dimensional surgical atlas developed by magnetic resonance imaging and micro-computed tomography (AP: -4.68, ML:  $\pm$  0.78, DV: -5.80 mm)<sup>34</sup>. Either a ferrule or a guide cannula (PlasticsOne) was subsequently placed at 50–500  $\mu$ m above the virus injection site(s) and fixed on the skull with a small amount of dental cement (Parkell). Ferrules and fibre-optic patch cords were either purchased from Doric Lenses or manufactured in our laboratory following the protocol provided by E. Boyden (MIT, <http://syntheticneurobiology.org/protocols/protocoldetail/35/9>). The virus-injected animals were housed individually in a reverse light/dark room during a 2 to 4-week recovery period, and then examined behaviourally and histologically.

## Behavioural tests

**Resident-intruder test.** Behavioural tests were initiated at 2 to 4 weeks post-surgery and repeated weekly for 2 to 5 weeks. Mouse cages were not cleaned for a minimum of 1 day until the behavioural test. The first test session on a given day began at 1–2 h after onset of the dark period. The virus-injected *Esr1*<sup>cre/+</sup> animals were briefly anaesthetized with isoflurane in a biosafety cabinet. The tip of a fibre-optic cable (200  $\mu$ m in core diameter, ThorLabs) was inserted to a depth just above the target brain region by introducing the cable into the brain through a guide cannula installed during surgery. For the ferrule-connector system, a ferrule patch cord was coupled to a ferrule on the head using a zirconia split sleeve (Doric Lenses). Mice were transferred to a test room illuminated with red lights and allowed to recover from anaesthetic for 20–30 min in their home cage placed in a rectangular Plexiglas test chamber fitted with infrared bulbs around the top as described previously<sup>32</sup>. The optical fibre was connected to a laser (473 nm for ChR2; 593 nm for eNpHR3.0; Shanghai Laser and Optics Century Co. and CrystaLaser) directly or via an optical commutator (Doric Lenses) to avoid twisting of the cable caused by the animal's movement. One to three intruders were individually introduced to an *Esr1*<sup>cre/+</sup> mouse in a testing session in a random order with respect to gender, with a 5–10 min interval between intruders. The strains of intruders were: intact males (BALB/c, 129S6/EvSv, and C57BL/6), castrated males (BALB/c), and intact non-hormone primed females (BALB/c and C57BL/6). After a testing session, *Esr1*<sup>cre/+</sup> animals were uncoupled from the fibre-optic cable and returned to a housing room.

**ChR2-mediated activation.** After the introduction of an intruder, a virus-injected animal was observed for 3–5 min to assess baseline behavioural responses towards an intruder, and then photostimulation was applied to the animal repeatedly by varying the irradiance, frequency, or duration of photostimulation, as well as the distance and the orientation of two animals at the onset of photostimulation. The intervals between photostimulation trials were >2.5 min. The frequency and duration of photostimulation were controlled using an Accupulse Generator (World Precision Instruments) or an Isolated Pulse Stimulator (A-M Systems). Laser power was controlled by dialing an analogue knob on the power supply of the laser sources. The control and experimental animals were processed in a random order.

One to three days after the final behavioural assay, the mouse was transcardially perfused with 4% paraformaldehyde, and the brain was histologically analysed to confirm viral expression in the target region, and ascertain the location of guide cannula or ferrule. Animals showing no detectable viral expression in the target region were excluded from statistical analysis. In some experiments, animals were photostimulated with a train of 473 nm light (20 ms-pulse, 20 Hz, 30 s min<sup>-1</sup> for 20 min) 60 min before perfusion in the absence of an intruder at an intensity which had evoked a behavioural phenotype in the final testing session. Then, brain sections were labelled for c-Fos to identify optogenetically activated cells.

In addition to close investigation, mounting and attack, photostimulation occasionally evoked a 'cornering' behaviour in some ChR2-expressing animals, in tests performed after short times of viral incubation (see Supplementary Note 3 for further information).

**eNpHR3.0-mediated silencing.** *Esr1*<sup>cre/+</sup> males expressing eNpHR3.0 or control mCherry were introduced to one to four male and female intruders, respectively, in 2–3 acclimation sessions without photostimulation to assess baseline aggression and reproductive behaviours of *Esr1*<sup>cre/+</sup> males as well as to augment aggressiveness and sexual behaviours in those animals. Animals that exhibited little aggression or reproductive behaviours during those initial sessions were excluded from subsequent testing sessions. During testing sessions, photostimulation (593 nm) ranging from 4.9–32.3 mW mm<sup>-2</sup> was delivered continuously for 10 s during male-male encounters and for 3 min during male-female encounters. To examine whether interruption of approach led to attack, strongly aggressive resident animals were chosen and stimulated when they were charging intruders >~5 cm from the intruder.

**Photostimulation intensity measurement.** Light power was measured from the tip of a ferrule connected to a ferrule patch cord before being installed in the brain (the ferrule-connector system) or from the tip of optical fibre (the guide cannula system) at different laser output settings, using an optical power and energy meter and a photodiode power sensor (ThorLabs). Irradiance was then calculated using the brain tissue light transmission calculator provided by the Deisseroth laboratory (<http://www.stanford.edu/group/dlab/cgi-bin/graph/chart.php>) using laser power measured at the tip and the distance from the tip to the target brain region measured by histology.

**Behavioural annotation.** Behavioural testing sessions were videotaped either from the side of the cage using Nero Vision and a camcorder (Sony), or simultaneously from both the side and top of the cage using StreamPix 5 (Norpix) and two scan cameras (Basler) with an infrared lens (Tamron) at a frame rate of 15–30 Hz. The camcorder and cameras were connected to a computer using IEEE 1394 FireWire cables. Behavioural annotation was carried out manually using custom software written in MATLAB as described previously<sup>32</sup>. An individual blind to the experimental

design scored behaviour on a frame-by-frame basis. The animals that exhibit no viral expression in a target brain region were excluded from analyses.

**Histology.** *In situ* hybridization (ISH) was carried out following the Allen Institute's ISH protocol (<http://help.brain-map.org/display/mousebrain/Documentation>)<sup>35</sup>. *In situ* probes for *Esr1* and *Cre* were generated with the following primer sets: *Cre* probe, 5'-ccaatttactgaccgtaccca-3' and 5'-tatttacattggccagccacc-3'; *Esr1* probe, 5'-taagaatacgccctgcctg-3' and 5'-acagtgtacgcaggagacagaa-3'.

For immunohistochemistry, animals were anaesthetized with ketamine and xylazine, and then transcardially perfused with 10 ml phosphate-buffered saline (PBS), followed by 10 ml ice-cold 4% paraformaldehyde in 0.1 M phosphate buffer, pH 7.4. Dissected brains were post-fixed for 1–3 h in 4% paraformaldehyde in 0.1 M phosphate buffer, pH 7.4 at 4 °C and transferred to 15% sucrose in 0.1 M phosphate buffer, pH 7.4. After overnight incubation at 4 °C, brains were frozen in Tissue-Tek O.C.T. embedding medium (Sakura). Coronal brain sections were cut at 30 µm using a cryostat (Leica Biosystems). Brain sections were rinsed briefly with phosphate-buffered saline. After blocking in 5% normal serum from host species where second antibody was generated from (Jackson ImmunoResearch), slides were treated with primary antibodies in 1% normal serum/0.3% Triton X-100/PBS overnight at 4 °C, followed by secondary antibody treatment at room temperature for 2 h. Sections were counterstained with NeuroTrace fluorescent Nissl stains (Invitrogen, N-21483, 1:100) or DAPI (Invitrogen, D3571, 300 nM). The primary antibodies used in this study are: rabbit anti-*Esr1* (Santa Cruz Biotechnology, sc-542, 1:200) and goat anti-*c-Fos* (Santa Cruz Biotechnology, sc2-g, 1:500). The fluorophore-conjugated secondary antibodies are: Alexa goat anti-rabbit (Invitrogen, A-11011, 1:500) and Alexa donkey anti-goat (Invitrogen, A-11055, 1:500). Fluorescent images were acquired using a confocal microscope (FluoView FV1000, Olympus). The number of fluorescent cells was counted manually as well as using MetaMorph Image Analysis Software (Molecular Devices). To detect the expression of *Esr1* and *c-Fos* in the VMHvl of male brains (Extended Data Fig. 1h–v), 40 µm free-floating brain sections were incubated with rabbit anti-*Esr1* (Santa Cruz Biotechnology, 1:1,000) and goat anti-*c-Fos* (Santa Cruz Biotechnology, 1:1,000) antibodies in 10% normal donkey serum/0.3% Triton X-100/PBS for 72 h on a rocking shaker at 4 °C, following blocking in 10% normal donkey serum for 1 h at room temperature. Brain sections were washed three times with PBS for 10 min each, and then incubated with Alexa donkey anti-rabbit IgG (Invitrogen, 1:500), Alexa donkey anti-goat IgG (Invitrogen, 1:500), and NeuroTrace fluorescent Nissl stains (Invitrogen, 1:200) in 10% normal donkey serum/0.3% Triton X-100/PBS for 2 h at room temperature. After washing with PBS 3 times for 10 min each, brain sections were mounted on slides.

**Electrophysiological recordings of acute hypothalamic slices.** All procedures for preparing acute brain slices and whole-cell recordings with optogenetic stimulations were carried out as described previously<sup>36,37</sup>. *Esr1*<sup>cre/+</sup> males were injected into VMHvl with a Cre-dependent AAV5 encoding ChR2-EYFP (AAV5.EF1 $\alpha$ .FLEX.ChR2-EYFP) or a Cre-dependent AAV2 encoding eNpHR3.0-mCherry (AAV2.EF1 $\alpha$ .FLEX.eNpHR3.0-mCherry) in a volume of 300 nl. After a 3–4-week viral incubation, coronal sections including the VMH were cut at 300 µm using a vibratome (VT-1000S, Leica Microsystems) in ice-cold cutting solution (composition in mM: 234 sucrose, 28 NaHCO<sub>3</sub>, 7 dextrose, 2.5 KCl, 7 MgCl<sub>2</sub>, 0.5 CaCl<sub>2</sub>, 1 sodium ascorbate, 3 sodium pyruvate and 1.25 NaH<sub>2</sub>PO<sub>4</sub>, oxygenated with 95% O<sub>2</sub>/5% CO<sub>2</sub>). Slices were then incubated in artificial cerebrospinal fluid (ACSF; composition in mM: 119 NaCl, 25 NaHCO<sub>3</sub>, 11 d-glucose, 2.5 KCl, 1.25 MgCl<sub>2</sub>, 2 CaCl<sub>2</sub> and 1.25 NaH<sub>2</sub>PO<sub>4</sub>, aerated with 95% O<sub>2</sub>/5% CO<sub>2</sub>) at 32 °C for at least one hour, and recorded at room temperature (20–25 °C). Cells expressing a virally-encoded fluorescent marker (ChR2-EYFP and eNpHR3.0-mCherry) were visualized by infrared differential interference contrast and fluorescence video microscopy (Olympus BX51). Whole-cell current clamp recordings were performed with a MultiClamp 700B amplifier and Digidata 1440A (Molecular Devices). The patch-clamp electrode (5–8 MΩ) was backfilled with an intracellular solution (composition in mM: 125 potassium gluconate, 10 KCl, 10 HEPES, 1 EGTA, 4 Mg-ATP, 0.3 Na<sub>2</sub>GTP, and 10 sodium phosphocreatine, pH 7.25, 280–300 mosM). Data were sampled at 10 kHz, filtered at 3 kHz, digitized and analysed with pClamp10 software (Molecular Devices). Photostimulation (ChR2, 473 nm, 2-ms pulses; eNpHR3, 532 nm, continuous; CrystaLaser) was applied to the hypothalamic slices from the tip of an optical fibre (200 µm in core diameter; ThorLabs) located at the dorsolateral edge of the VMHvl (~700 µm from the centre of VMHvl). The spike fidelity in ChR2-expressing *Esr1*<sup>+/+</sup> neurons was measured by counting the number of light pulses that successfully evoked action potentials upon 473 nm photostimulation (2- or 20-ms pulses) at different frequencies (2, 5, 10, 20, and 40 Hz).

**Calcium imaging of acute hypothalamic slices.** *Esr1*<sup>cre/+</sup> males were injected into the VMHvl with a mixture of AAV5 encoding Cre-dependent ChR2-EYFP (AAV5.EF1 $\alpha$ .FLEX.ChR2-EYFP), AAV2 encoding Cre-dependent nuclear mCherry (AAV2.EF1 $\alpha$ .FLEX.nuclear mCherry), and AAV1 encoding GCaMP6s<sup>38</sup> (AAV1.Syn.GCaMP6s), in a volume of 300 nl (2:1:1 volume ratio). In control experiments,

the same viral mixture without AAV5.EF1 $\alpha$ .FLEX.ChR2-EYFP was injected. After a 3.5-week viral incubation, acute hypothalamic slices were prepared from the virus-injected mice similar to the procedures described above in section Electrophysiological recordings of acute hypothalamic slices. Calcium imaging was carried out using a two-photon laser-scanning microscope (Ultima, Prairie Instruments Inc.) with a 20 × /1.0-NA XLUMPlanFL/N water-immersion objective (Olympus). The Ti:sapphire laser was tuned to 940 nm (power: 10 mW), and 512 × 512 pixel images were acquired at 1.3 Hz frame rate (1.6 µs dwell time per pixel) through 525/50 nm emission filter. Photostimulation (445 nm, 2-ms pulse, 20 Hz) was applied to the dorsolateral edge of the VMHvl (~700 µm from the centre of VMHvl) at different intensities (4.8, 14.5, 30.2, 4.8 mW) with 3-min intervals between photostimulation trials. Data were analysed using the custom software written in MATLAB (VivoViewer) as described previously<sup>39</sup>. In brief, the raw fluorescence images were smoothed using a two-dimensional Gaussian filter. We then calculated the fluorescence changes relative to the baseline ( $\Delta F/F = (F - F_0)/F_0$  where  $F_0$  is the average pixel intensity in the first 3–6 baseline frames of the experiment) in each GCaMP6s<sup>+</sup> cell (detected manually). Because the 445-nm photostimulation used to activate ChR2 could penetrate through the emission filter and affect  $\Delta F/F$ ,  $\Delta F/F_{\text{peak}}$  and  $\Delta F/F_{\text{area}}$  during the photostimulation periods were excluded from analysis. 'Activated cells' for Fig. 4r were operationally defined as cells showing an increase in  $\Delta F/F > 5$  standard deviations from baseline  $\Delta F/F$  measured from 5 frames before the first photostimulation.

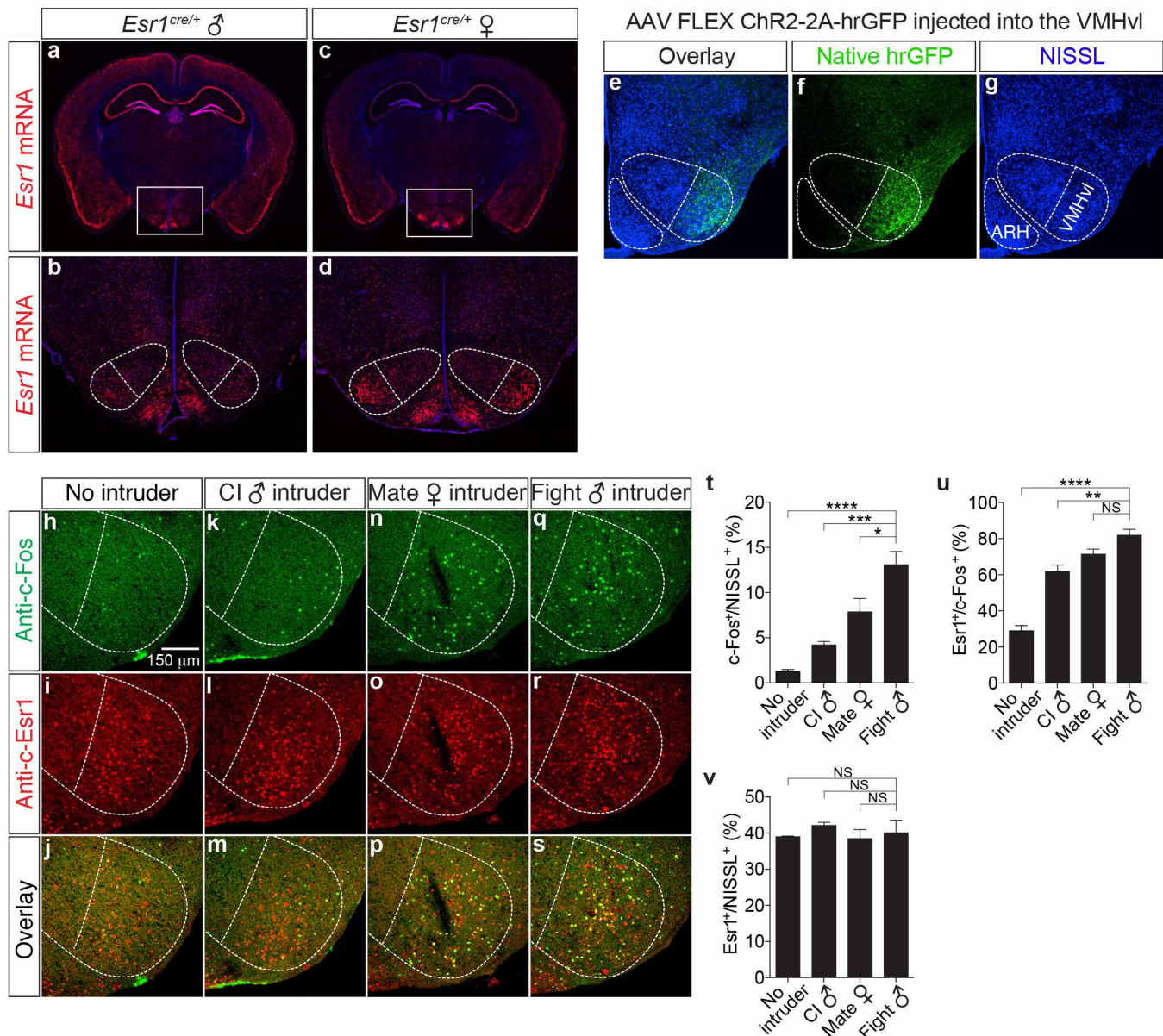
**In vivo electrophysiological recordings.** *In vivo* extracellular recordings were carried out as described previously with modifications<sup>32</sup>. A custom-built optrode was used to obtain multi-unit activity, comprising a 62.5 µm core optical fibre and a tungsten microwire bundle. The mouse line (*Esr1*<sup>cre/+</sup>) and viral expression of ChR2 (AAV2.EF1 $\alpha$ .FLEX.ChR2-F2A-nuclear hrGFP) were identical to that used in the behavioural experiments. Photostimulation parameters for a given optrode were calibrated before implantation so that the transmitted light would irradiate the brain tissue at 1.0 to 1.5 mW mm<sup>-2</sup>, measured under constant illumination. Recordings were obtained using the same photostimulation parameters as those used in the behavioural experiments, that is, at 20 Hz with 20 ms pulse-width, and also with 10 ms and 2 ms pulse-widths so as to determine any linearity or trends between the stimulation parameters and response (Extended Data Fig. 2a). Neural activity was recorded over a baseline period of 30 s, followed by a photostimulation period of 30 s, followed by a post-stimulation/recovery period of 60 s. 5 trials were obtained for each recording site and the photostimulation periods between two successive trials were at least 2 min apart.

Extracellular recordings are traditionally resolved into the activity profiles of single units obtained through spike-sorting, where variations in spike waveform properties are used to assign individual spikes to single units. However, photostimulation has been demonstrated to deform spike waveforms<sup>40</sup> and the variance in spike waveform shape under 10 ms and 20 ms photostimulation pulse-widths greatly hindered the assignment of photostimulated spikes to individual units. To overcome this limitation all spikes recorded at a single microwire electrode (crossing a threshold two standard-deviations over baseline, spike wavelength around 1 ms and interspike interval greater than 2 ms) were grouped together into a multi-unit. Hardware and software provisions for eliminating photoelectric artefact were used<sup>41</sup>. Acquired data was analysed post hoc in Matlab using custom-written scripts. Peri-stimulus time-histograms were constructed using bins of 100 ms and plotted with Gaussian smoothing.

We used a two-step process to determine that the multi-units recorded were within the VMHvl. First we shortlisted multi-units where the average activity during the entire period of 30 s using 2 ms pulses and 20 Hz photostimulation (P) was greater than one standard deviation (S) over the average baseline (B) activity (P > B + S). Next the implanted animals were placed in a resident–intruder assay and the multi-units were further shortlisted based on whether constituent single units were identified to be strongly responsive during mating or aggressive epochs. Overall, from a total of 22 recording sites only 12 multi-units were determined to be localized within the VMHvl.

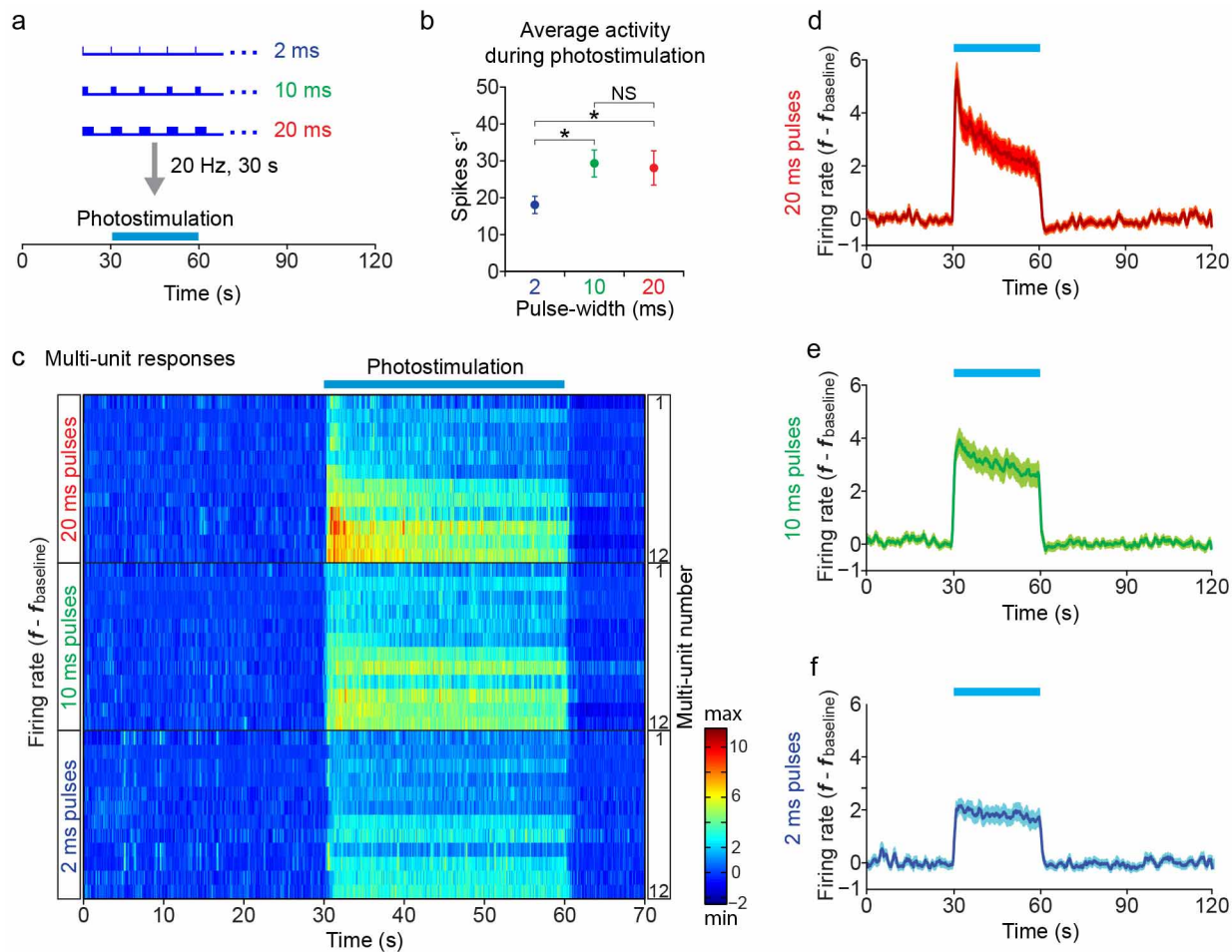
31. Wu, Y., Wang, C., Sun, H., LeRoith, D. & Yakar, S. High-efficient FLpo deleter mice in C57BL/6J background. *PLoS ONE* **4**, e8054 (2009).
32. Lin, D. *et al.* Functional identification of an aggression locus in the mouse hypothalamus. *Nature* **470**, 221–226 (2011).
33. Harris, J. A., Oh, S. W. & Zeng, H. Adeno-associated viral vectors for anterograde axonal tracing with fluorescent proteins in nontransgenic and cre driver mice. *Curr Protoc Neurosci Chapter 1. Unit 1 20 21-18* (2012).
34. Chan, E., Kovacevic, N., Ho, S. K., Henkelman, R. M. & Henderson, J. T. Development of a high resolution three-dimensional surgical atlas of the murine head for strains 129S1/SvImJ and C57BL/6J using magnetic resonance imaging and micro-computed tomography. *Neuroscience* **144**, 604–615 (2007).
35. Lein, E. S. *et al.* Genome-wide atlas of gene expression in the adult mouse brain. *Nature* **445**, 168–176 (2007).
36. Haubensak, W. *et al.* Genetic dissection of an amygdala microcircuit that gates conditioned fear. *Nature* **468**, 270–276 (2010).
37. Atasoy, D., Betley, J. N., Su, H. H. & Sternson, S. M. Deconstruction of a neural circuit for hunger. *Nature* **488**, 172–177 (2012).

38. Chen, T. W. *et al.* Ultrasensitive fluorescent proteins for imaging neuronal activity. *Nature* **499**, 295–300 (2013).
39. Vrontou, S., Wong, A. M., Rau, K. K., Koerber, H. R. & Anderson, D. J. Genetic identification of C fibres that detect massage-like stroking of hairy skin in vivo. *Nature* **493**, 669–673 (2013).
40. Cohen, J. Y., Haesler, S., Vong, L., Lowell, B. B. & Uchida, N. Neuron-type-specific signals for reward and punishment in the ventral tegmental area. *Nature* **482**, 85–88 (2012).
41. Kvitsiani, D. *et al.* Distinct behavioural and network correlates of two interneuron types in prefrontal cortex. *Nature* **498**, 363–366 (2013).



**Extended Data Figure 1 | *Esr1* mRNA expression in *Esr1*<sup>cre/+</sup> male and female mice.** **a–d**, *In situ* hybridization for *Esr1* mRNA in *Esr1*<sup>cre/+</sup> male (**a, b**, red) and female (**c, d**, red) mice (Bregma  $\sim -1.65$  mm). **b, d** are the boxed areas in **a–c**. Note that the expression of *Esr1* mRNA in VMHvl (dotted outline) is higher in females than in males. **e–g**, Immunofluorescence showing that expression of a Cre-dependent hrGFP reporter expressed from a stereotactically injected AAV (**f**, green) is restricted to VMHvl, without detectable spillover expression in the nearby arcuate hypothalamic nucleus (ARH). **h–s**, Double labelling for behaviourally-induced c-Fos

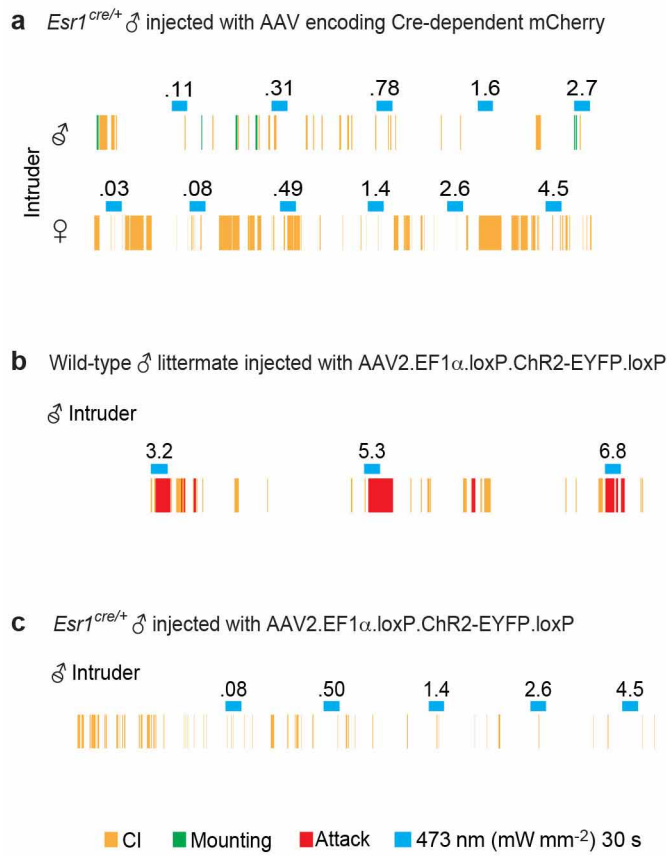
(**h, k, n, q**, anti-c-Fos, green) and *Esr1* (**i, l, o, r**, anti-Esr1, red) in wild-type male residents following a 30-min resident-intruder test with no (**h–j**,  $n = 3$ ), male (**k–m**, close investigation without attack,  $n = 4$ ; **q–s**, attack,  $n = 5$ ) or female (**n–p**, mating,  $n = 5$ ) intruders. **t–v**, Quantification of the fraction of total (NISSL<sup>+</sup>) cells that were c-Fos<sup>+</sup> following different behaviours (**t**), fraction of c-Fos<sup>+</sup> that were *Esr1*<sup>+</sup> for each behaviour (**u**), and fraction of NISSL<sup>+</sup> cells that are *Esr1*<sup>+</sup> (**v**) in VMHvl, quantified from data as illustrated in **h–s**. \* $P < 0.05$ , \*\* $P < 0.001$ , \*\*\* $P < 0.0001$ ; one-way ANOVA with Dunnett's multiple comparisons test.



### Extended Data Figure 2 | *In vivo* electrophysiological responses of Esr1<sup>+</sup> VMHvl neurons during photostimulation with 2, 10, and 20-ms pulses.

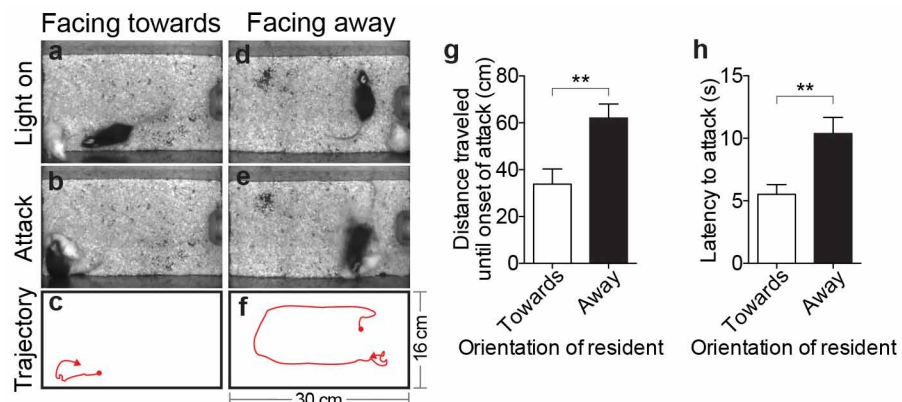
**a**, Photostimulation paradigm. Extracellular recordings were obtained from Esr1<sup>+</sup> VMHvl neurons expressing AAV2 Cre-dependent ChR2 in solitary, awake behaving animals using a modification of a 16-wire electrode bundle micro-drive<sup>31</sup> containing an integrated optic fibre. Following a 30-s baseline measurement, photostimulation trials were performed (473 nm, 20 Hz, blue bars) for 30 s using three different pulse-widths (2 ms, 10 ms, and 20 ms). Five trials, each 2 min in length, were recorded for each pulse-width (see c). **b**, Mean firing rate changes averaged across 12 multi-units (5 trials per unit) in VMHvl during 30-s photostimulation periods. 2 ms,  $17.98 \pm 2.35$  spikes per s, 10 ms,  $29.26 \pm 3.67$  spikes per s, and 20 ms,  $28.07 \pm 4.65$  spikes per s.

\*P < 0.05, Wilcoxon rank sum test. **c**, Spiking responses of 12 multi-unit recording channels in VMHvl. Each raster plot represents the average of five trials per channel per pulse-width (2, 10 or 20 ms), arranged in order of response magnitude. The arrangement is the same for the three pulse widths (2 ms, 10 ms and 20 ms). **d–f**, Peri-stimulus time histograms (PSTHs) illustrating mean firing rate changes averaged over the 12 multi-units shown in c, for photostimulation trials using 20 ms (d), 10 ms (e), or 2 ms (f) light pulse-widths. Data are mean  $\pm$  s.e.m. See also main Fig. 2d, which presents whole-cell patch-clamp recordings from Esr1<sup>+</sup> neurons in VMHvl acute slice preparations, indicating that spike fidelity is close to 100% and statistically indistinguishable between 2 ms and 20 ms light pulse-widths.



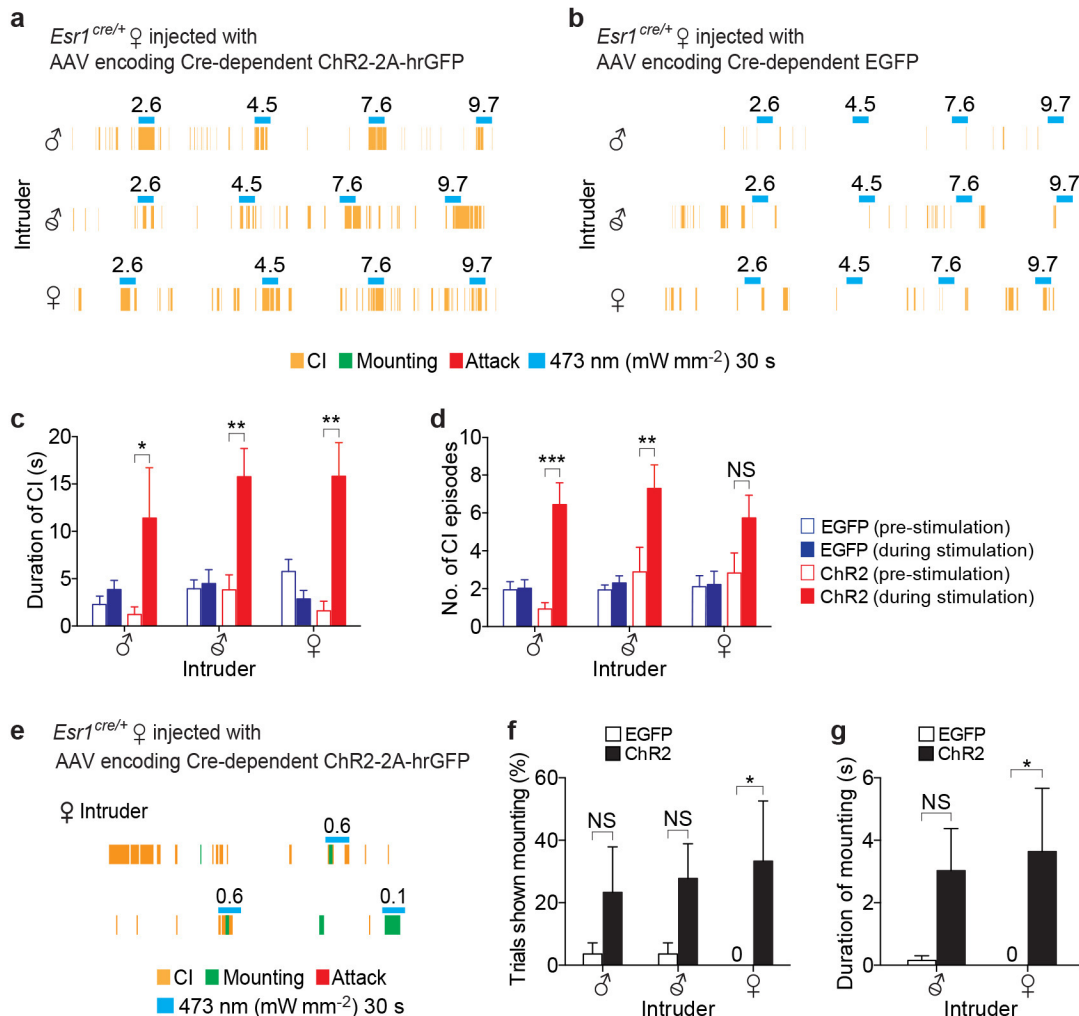
**Extended Data Figure 3 | Photostimulation of *Esr1*<sup>+</sup> VMHvl neurons expressing mCherry or *Esr1*<sup>-</sup> VMHvl neurons expressing ChR2 fails to evoke aggression.** **a**, Animals expressing Cre-dependent mCherry virus in VMHvl fail to show aggression during photostimulation. Representative raster plot showing episodes of close investigation (CI; yellow ticks), mounting (green ticks) or attack (red ticks) in an mCherry-expressing *Esr1<sup>cre/+</sup>* male. No attacks are evoked towards either a castrated male (upper plot) or an intact unreceptive female (lower plot) during photostimulation trials (blue bars; 473 nm, 20 ms pulses, 20 Hz, 30 s; numbers indicate mW mm<sup>-2</sup>). **b, c**, Activation of the

non-*Esr1*-expressing subpopulations of VMHvl neurons is insufficient to evoke aggression. Representative raster plots illustrating photostimulation-evoked behavioural responses towards a castrated male by a wild-type (**b**) or an *Esr1<sup>cre/+</sup>* (**c**) mouse injected with the ‘Cre-out’ AAV2 containing a floxed ChR2 coding sequence (Fig. 2r). Attack (red; 3.2–6.8 mW mm<sup>-2</sup>) was elicited during photostimulation trials (blue bars) in wild-type males, indicating that the floxed ChR2 construct is effective in the absence of Cre, whereas no behaviour was evoked in *Esr1<sup>cre/+</sup>* males where ChR2 is expressed in *Esr1*<sup>-</sup>, but not in *Esr1*<sup>+</sup>, neurons.



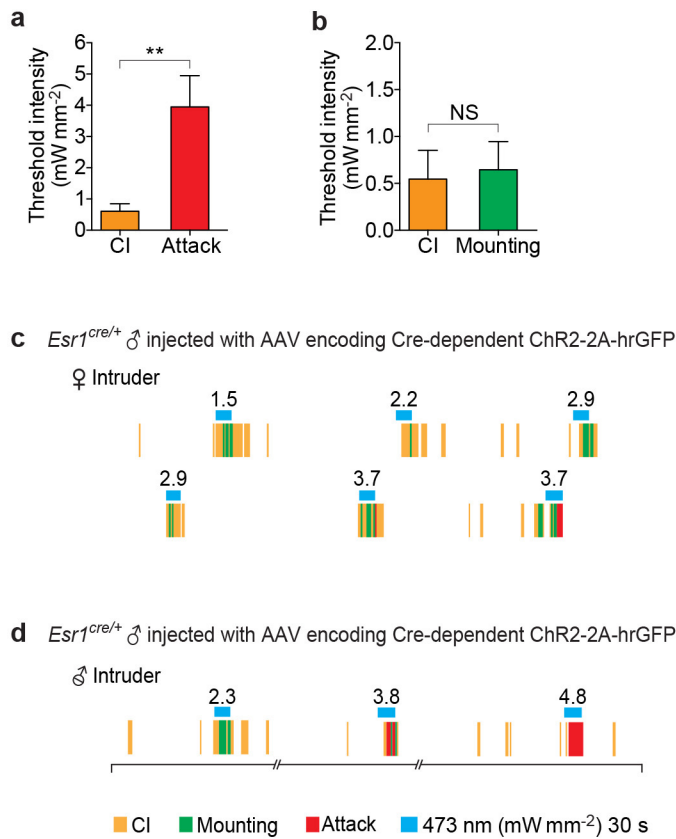
**Extended Data Figure 4 | Latency to attack depends on the initial orientation of the resident with respect to the intruder at the time of photostimulation.** **a, b, d, e,** Video stills illustrating initial position and orientation ('facing toward vs away') of a ChR2-expressing *Esr1<sup>cre/+</sup>* male (black) towards a castrated male intruder (white) at the onset of photostimulation (**a, d**) and at the initiation of evoked attack (**b, e**). **c, f,** trajectory plots showing the paths taken by the *Esr1<sup>cre/+</sup>* males from the onset of photostimulation (red dots) to the onset of attack (red arrowheads). Cage dimensions indicated in **f**. **g, h,** Quantification of distance travelled from onset of photostimulation to attack (**g**) and latency to attack (**h**), from data in **a–f** ( $n = 11$ ,  $**P < 0.01$ , Mann–Whitney U-test). Note that if the resident is initially facing away from the intruder (**d–f**), the latency to attack is longer (**h**) because the resident initially moves in the direction that it was facing (**f**) and does not attack until it encounters the intruder at close range. Data are mean  $\pm$  s.e.m.  $n =$  number of animals.

arrowheads). Cage dimensions indicated in **f**. **g, h,** Quantification of distance travelled from onset of photostimulation to attack (**g**) and latency to attack (**h**), from data in **a–f** ( $n = 11$ ,  $**P < 0.01$ , Mann–Whitney U-test). Note that if the resident is initially facing away from the intruder (**d–f**), the latency to attack is longer (**h**) because the resident initially moves in the direction that it was facing (**f**) and does not attack until it encounters the intruder at close range. Data are mean  $\pm$  s.e.m.  $n =$  number of animals.

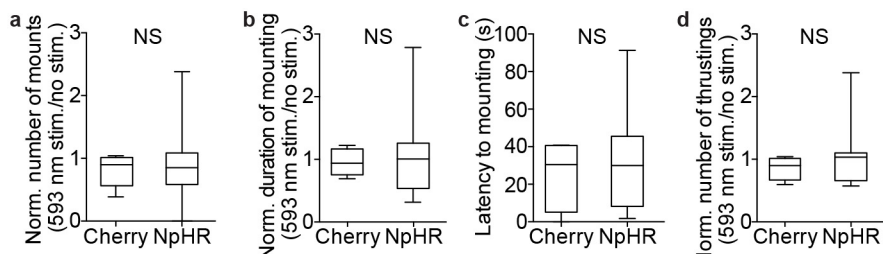


**Extended Data Figure 5 | Photostimulation of VMHvl *Esr1*<sup>+</sup> neurons in females evokes close investigation and mounting.** **a, b,** Representative raster plots illustrating photostimulation-evoked behaviours in *Esr1<sup>cre/+</sup>* females expressing either ChR2 (**a**) or EGFP (**b**) in VMHvl towards an intact male (upper), a castrated male (middle), or an intact female (lower). Note that CI (yellow) is augmented during photostimulation in the animal expressing ChR2, but not in the animal expressing EGFP. **c, d,** Quantification of CI by *Esr1<sup>cre/+</sup>* females expressing EGFP (blue bars;  $n = 4$  per intruder) or ChR2 (red bars;  $n = 3$  per intruder) during 30 s before photostimulation (open symbols) vs during 30 s photostimulation period (solid symbols). \* $P < 0.05$ , \*\* $P < 0.01$ ,

\*\*\* $P < 0.001$ ; two-way ANOVA with Tukey's multiple comparisons test. **e,** Raster plot illustrating that photostimulation of *Esr1<sup>cre/+</sup>* female expressing ChR2 evokes mounting (green), but failed to elicit male-like aggression. **f, g,** Quantification of mounting parameters by *Esr1<sup>cre/+</sup>* females expressing EGFP (open bars;  $n = 4$  per intruder) or ChR2 (black bars;  $n = 3$  per intruder) towards the indicated intruders. Two-way ANOVA with Tukey's multiple comparisons test, \* $P = 0.02$  (**f**) and \* $P = 0.03$  (**g**) without correction for multiple comparisons, but not significant when corrected ( $P = 0.07$  (**f**) and  $P = 0.06$  (**g**)). Data are mean  $\pm$  s.e.m.  $n$  = number of animals.

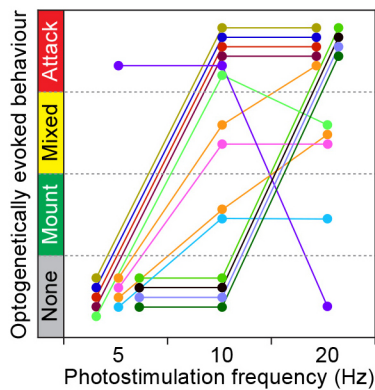


**Extended Data Figure 6 | CI and mounting are evoked at lower photostimulation intensities than attack.** **a, b**, The average threshold intensity of photostimulation that evokes close investigation (CI) is similar to that required to evoke mounting (b), but significantly lower than that required to evoke attack (a). Data represent ChR2-expressing *Esr1<sup>cre/+</sup>* males that exhibited CI and attack (a,  $n = 12$  per group) or CI and mounting (b,  $n = 9$  per group) in a given test session. \*\* $P < 0.01$ ; Mann–Whitney U-test. Data are mean  $\pm$  s.e.m.  $n$  = number of animals. **c, d**, Raster plot from a test session with the same resident male, showing that activation of VMHvl *Esr1<sup>+</sup>* neurons elicits mounting and/or attack towards a castrated male intruder, dependent upon the intensity of photostimulation. **c**, A raster plot illustrating the experiment shown in Supplementary Video 6. Mounting (green) was elicited in a ChR2-expressing *Esr1<sup>cre/+</sup>* male towards an unreceptive intact female during photostimulation trials (blue bars; 30 s). Note that mounting was followed by attack (red) in the high intensity photostimulation trials ( $3.7 \text{ mW mm}^{-2}$ ). **d**, A raster plot illustrating a shift in behavioural responses from mounting to attack towards a castrated male intruder dependent upon photostimulation intensity (see Fig. 4a for the behavioural shift towards a female intruder). Note that time line is not continuous at the breakage in the line under rasters.



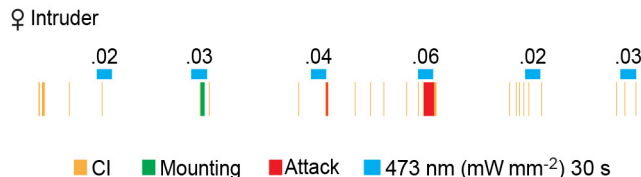
**Extended Data Figure 7 | Optogenetic silencing of VMHvl *Esr1*<sup>+</sup> neurons does not affect reproductive behaviours towards females.**  
**a–d,** Quantification of female-directed mating behaviours during photostimulation of *Esr1*<sup>cre/+</sup> males expressing mCherry ( $n = 4\text{--}5$ ) or eNpHR3.0 ( $n = 14\text{--}17$ ). **a, b, d,** Parameters of reproductive behaviours

during photostimulation trials (3 min) were normalized to those during non-stimulated periods. **c,** The latency from the onset of photostimulation to the first mounting. n.s., not significant; Mann–Whitney U-test. Data are mean  $\pm$  s.e.m.  $n$  = number of animals.

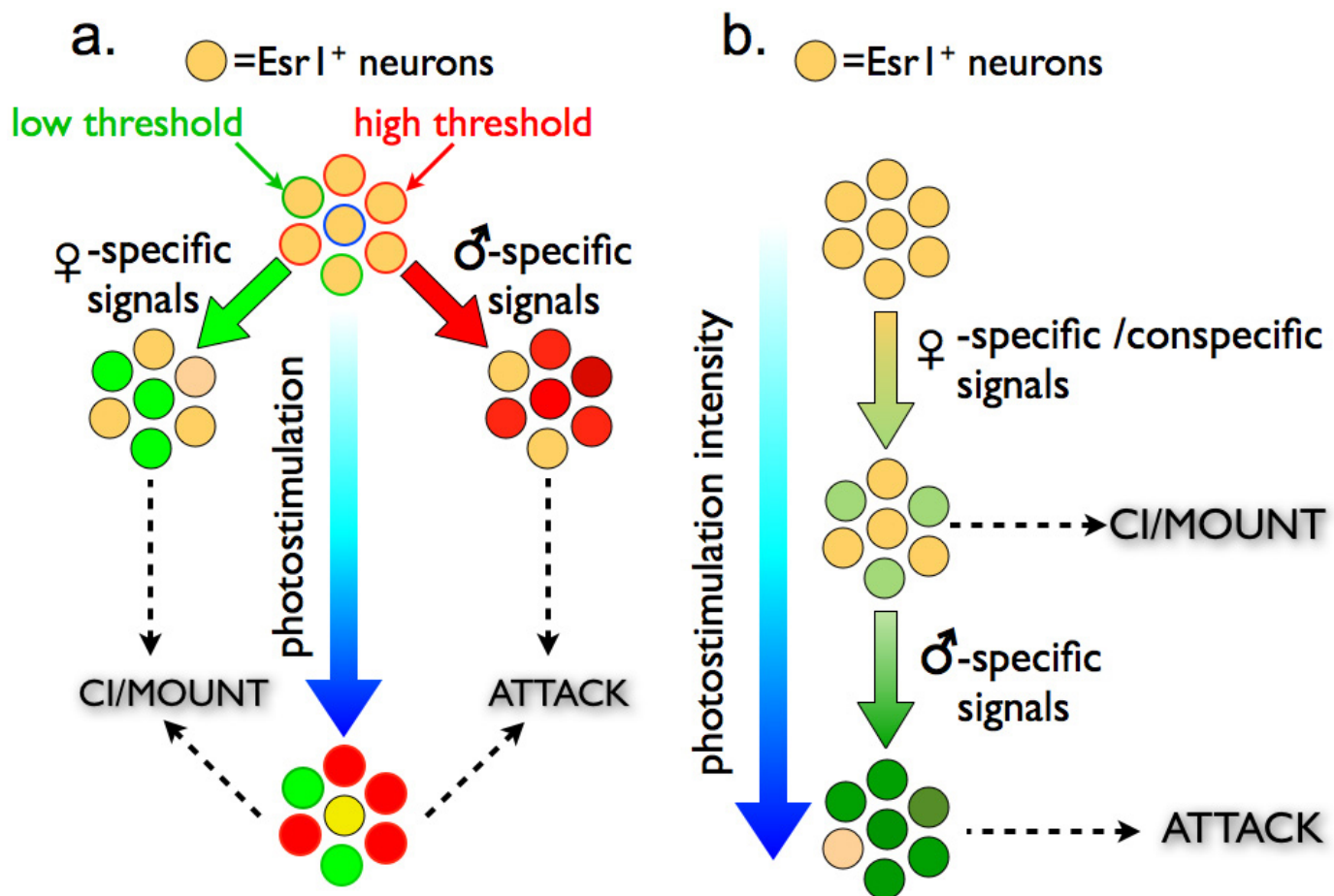


**Extended Data Figure 8 | Relationship between behavioural response and photostimulation frequency.** Behaviours evoked by optogenetic activation of ChR2-expressing *Esr1<sup>cre/+</sup>* males at the indicated photostimulation frequencies are plotted (5, 10, and 20 Hz). Different photostimulation intensities were applied in different episodes (coloured lines). In each episode, photostimulation frequency was varied at a fixed intensity. Only 2/14 stimulation episodes (orange) exhibited a behavioural shift from mounting to mixed to attack behaviours with increasing photostimulation frequency. Data from  $n = 11$  animals.

*Esr1*<sup>cre/+</sup> ♂ injected with AAV encoding Cre-dependent ChR2-2A-hrGFP



**Extended Data Figure 9 | An example of hysteresis.** A representative raster plot illustrating a shift from mounting ( $0.3 \text{ mW mm}^{-2}$ ) to attack ( $0.6 \text{ mW mm}^{-2}$ ) with increasing photostimulation intensity. Note that once attack was elicited, reducing the photostimulation intensity back to  $0.3 \text{ mW mm}^{-2}$  no longer evoked mounting, but simply failed to elicit attack. Whether this hysteresis is intrinsic to the animal, or represents a form of conditioning, is not clear.



Extended Data Figure 10 | Two alternative models to explain how activation of  $\text{Esr1}^+$  neurons in VMHvl can promote mounting and attack depending on conditions. See Supplementary Note 2.